Impact of alteration corridors on karst reservoir organisation and evolution of groundwater flow path: An example from the southern border of the Larzac Causse, southern France

Céline Baral, Michel Séranne, Hubert Camus, Johan Jouves

BSGF - Earth Sciences Bulletin 2024, 195, 4
© C. Baral *et al.*, Published by EDP Sciences 2024
https://doi.org/10.1051/bsgf/2023017

BSGF
Earth Sciences Bulletin
Available online at:
www.bsgf.fr

Open Access

Impact of alteration corridors on karst reservoir organisation and evolution of groundwater flow path: An example from the southern border of the Larzac Causse, southern France

Céline Baral[1,2,*], Michel Séranne[2], Hubert Camus[1] and Johan Jouves[1]

[1] Cenote, 1 chemin de Valdegour, 30900 Nîmes, France
[2] Géosciences Montpellier, Université de Montpellier–CNRS, Montpellier, France

Received: 24 October 2023 / Accepted: 18 December 2023 / Publishing online: 27 March 2024

Abstract – All the features of karstic reservoirs result from the chemical and/or mechanical erosion of an initial rock volume, which modifies the initial petrophysical properties (*i.e.*, porosity and permeability). The spatial distribution and organisation of the karst system in a carbonate massif are often overlooked in studies on karst hydrological functioning. However, these parameters are key to understand and accurately model dynamic flow. This contribution aims at characterising the nature and impact of alteration corridors on the organisation and evolution of the karstic reservoir and its present-day functioning. We focus on characterising the specific impact of the late onset of pocket valley regressive erosion on the organisation of the present-day drainage system. We used a 3D approach to correlate field observations on the surface and in caves, with remote sensing. The expression of alteration corridors is analysed in a 40 km^2 area on the southern border of the Larzac Causse. This Jurassic carbonate massif is affected over its entire thickness by a network of vertically elongated alteration corridors containing dissolution-collapse breccia, mainly oriented in a N-S direction. Ghost-rock karstification played a significant part in the karstic reservoir structure and evolution. Alteration corridors result from the in-situ dissolution of the bedrock along an initial jointing pattern. The dissolution-collapse breccia corridors correspond to ghost-rock corridors selectively emptied of their alterite, under the effect of a hydraulic gradient. The vertically elongated structure of alteration corridors that cross-cut the Jurassic sequence enables fluid circulation from an upper to a lower aquifer, which were initially separated by a Toarcian marly seal unit. The subsequent initiation of pocket valleys led to the rapid evacuation of the residual alterite contained in ghost-rock corridors, under the influence of gravity. These alteration corridors determine the position of present-day pocket valley springs and enhance the regressive erosion dynamics, that progressively capture a north-east flowing watershed (Vis River). Finally, residual alterites are evacuated below the overflow spring altitude during high-flow events by flooding/dewatering of galleries. Such mechanisms of alterite evacuation provide insight into i) the part of the karstic reservoir that is connected to the spring, and ii) the dynamics of the associated flows. This study suggests that corridor networks constitute a substantial volume of porous and permeable materials that plays a major role in the present-day groundwater flow path. Such features should be considered valuable drilling targets for water exploration when located below the piezometric level.

Keywords: palaeokarst / ghost-rock karstification / dissolution breccia / pocket valley / speleogenesis / water resources

Résumé – Impact des couloirs d'altérations sur l'organisation des réservoirs karstique et l'évolution des chemins de circulation d'eau souterraine: Un exemple de la bordure sud du causse du Larzac, sud de la France. Le réservoir karstique est constitué de l'ensemble des discontinuités résultant de l'altération chimique et/ou mécanique d'un volume de roche initial qui conduisent à la modification de ses propriétés pétrophysiques initiales (porosité, perméabilité). Les études sur le fonctionnement hydrologique des systèmes karstiques ne prennent pas souvent en compte la géométrie et la distribution spatiale de ce dernier. Or, ces paramètres sont clés pour la compréhension et la modélisation cohérente des dynamiques de drainage en profondeur. Cette étude vise à caractériser le développement, la nature et l'impact des couloirs d'altérations sur la structuration du réservoir karstique et son fonctionnement actuel. Cette étude caractérise

*Corresponding author: celine.baral@cenote.fr

l'impact spécifique de la mise en place tardive des reculées karstiques sur l'organisation du système de drainage actuel. Nous utilisons une approche 3D permettant de corréler les observations de terrain, en surface et dans les réseaux spéléologiques, avec les données de télédétection. L'expression des couloirs d'altération est analysée dans une zone de 40 km^2 sur la bordure sud du causse du Larzac. Le massif carbonaté Jurassique est affecté sur toute son épaisseur par un maillage de couloirs d'altération verticaux contenant des brèches de dissolution-effondrement, principalement orientés N-S. Le processus de karstification par fantômisation est identifié comme jouant un rôle majeur dans la géométrie et l'évolution du réservoir karstique. Les couloirs d'altérations résultent de la dissolution in-situ de l'encaissant le long d'un maillage de fractures préexistantes. Les couloirs de dissolution-effondrement correspondent à des couloirs de fantômes débourrés de manière sélective sous l'effet d'un gradient hydraulique. Leur géométrie verticale permet la circulation de fluide entre les aquifères supérieur et inférieur, initialement séparés par l'imperméable marneux du Toarcien. L'initiation et le développement des reculées karstiques en bordure de plateau provoque l'évacuation rapide des altérites résiduelles contenues dans les couloirs d'altération, sous l'effet d'un écoulement gravitaire. Les couloirs d'altération contrôlent la position des sources karstiques actuelles, et favorisent la dynamique d'érosion régressive des reculées qui capturent progressivement le bassin d'alimentation voisin drainé vers le NE (canyon de la Vis). Enfin, les altérites résiduelles sont évacuées sous le niveau de la source de trop plein par un mécanisme de mise en charge dans la zone épinoyée. Ces différents mécanismes d'évacuation renseignent sur la partie du réservoir sollicitée par une source ainsi que sur la dynamique de circulation associée. Cette étude montre que les réseaux de couloirs constituent un volume considérable de matériel poreux et perméable qui jouent un rôle important dans les circulations d'eau souterraines actuelles. Ces structures devraient être considérées comme des cibles intéressantes pour l'exploration d'eau souterraine.

Mots clés : paléokarst / fantômisation / brèche de dissolution / reculée karstique / spéléogénèse / ressource en eau

1 Introduction

The Mediterranean basin undergoes significant climatic and demographic pressure (Cramer *et al.*, 2018), inducing an increasing demand for freshwater, while the region records more frequent drought periods (Mathbout *et al.*, 2021; Vicente-Serrano *et al.*, 2014). Karstic aquifers play a crucial role in supplying freshwater in the south of France (Bakalowicz, 2010). However, they are vulnerable to contamination and challenging to manage because of their complex heterogeneity (Bakalowicz, 2005). Local authorities are urged to plan for future water needs, to identify potential water resources, and to establish protected areas to prevent aquifer pollution. In this context, assessing karstic areas in terms of water reservoir storage capacity and/or vulnerability has become a critical necessity (COST Action 620, 2004).

Many modelling approaches have focused on the hydrological functioning of karstic systems (Goldscheider and Drew, 2007; Hartmann *et al.*, 2014; Jeannin *et al.*, 2021; Pinault *et al.*, 2001; Tritz *et al.*, 2011) to predict their resources, vulnerability and impact of flooding events (De Waele and Gutiérrez, 2022; Ford and Williams, 2007; Malagò *et al.*, 2016). However, these general approaches fail to satisfactorily address the geometry and spatial distribution of the karstic network used by groundwater flow (Bakalowicz, 2005; Jourde *et al.*, 2018). Recent methods have been suggested to simulate karst geometry, using geostatistical approaches based on available data, which remain limited to fracturation, inlet/outlet points, inception horizon (Borghi *et al.*, 2012; Goldscheider and Drew, 2007; Luo *et al.*, 2021), and conduit geometry of the existing caves (Fournillon *et al.*, 2012). In order to assess underground water availability and to safely manage water resources in karstic provinces, it is pivotal to understand the spatial distribution of heterogeneities within the karstic reservoir.

Karstic reservoirs display specific geometries and organisations that are dependent on karstification processes, base-level changes, environmental parameters (De Waele and Gutiérrez, 2022; Ford and Williams, 1989), and are closely related to the geodynamical and geomorphological evolution of the carbonate massif (Bruxelles, 2001; Camus, 2003; Devos *et al.*, 1999; Hill and Polyak, 2020; Husson *et al.*, 2017, 2018). To identify the factors controlling karstic reservoir development, it is necessary to decipher the successive phases of karstification by analysing the long-term geological and geodynamic evolution of the carbonate massif (Audra and Palmer, 2015; Husson *et al.*, 2017, 2018). Understanding the successive phases of karstification, associated with their resulting specific structures, allows: i) to integrate the major steps of karstic reservoir organisation as controlling parameters, for the geostatistical simulation (Jouves *et al.*, 2017) and ii) to consider the inheritance of the previous phases of karst evolution. Therefore, providing time-related and quantitative structural data from natural analogues is key for making realistic predictions about the geometry and spatial distribution of karstic reservoirs (Husson *et al.*, 2018; Jouves, 2018; La Bruna *et al.*, 2021; Pisani *et al.*, 2022).

In this contribution, we focus on the specific characterisation, evolution and impact on groundwater flow of 'alteration corridors'. We define alteration corridors as corridor-shaped features resulting from the alteration of the initial rock volume by chemical dissolution or mechanical erosion processes. These structures may include "cave corridors" (Klimchouk *et al.*, 2016), "fracture corridor" (*e.g.*, Furtado *et al.*, 2022; La Bruna *et al.*, 2021; Li *et al.*, 2019) and "ghost-rock corridors" (Quinif, 2017). Ghost-rock corridors result from a two-step

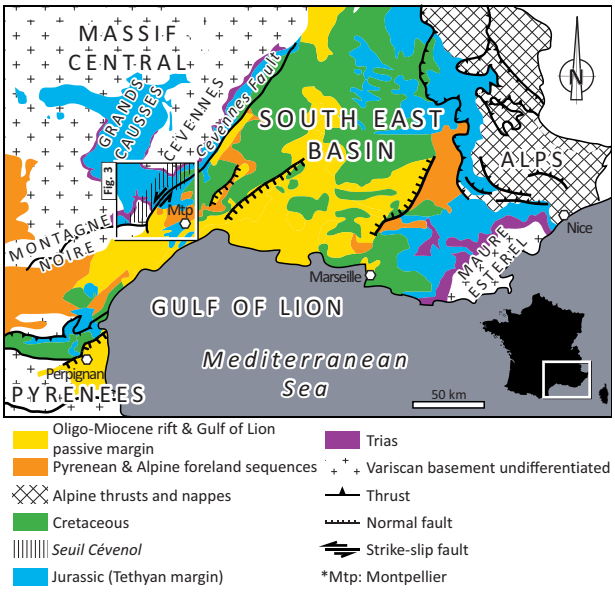

Fig. 1. Structural setting of southeastern France, synthesised from BRGM 1/10^6 scale map of France. The study area (corresponding to the location of Figure 3) is located on the western border of the Tethyan margin, on the Seuil Cévenol that constitutes a structural high separating the Grands Causses basin from the South-East Basin.

ghost-rock karstification process, which includes i) diffusive selective dissolution of a rock volume preserving its volume and structure and ii) evacuation of the undissolved particles (Quinif, 1999; Vergari, 1998). Ghost-rock features, characterised by enhanced porosity (up to 60%) and permeability (up to 10 Darcy) (Dubois *et al.*, 2014), favour fluid flows (Quinif and Bruxelles, 2011; Quinif and Maire, 2009) and underground water resources (Dandurand *et al.*, 2014, 2019). Ghost-rock corridors have been observed locally in caves (Quinif, 2017), in outcrops (Dandurand *et al.*, 2014, 2019), and quarries (Broughton, 2018; Kaufmann and Deceuster, 2014; Quinif and Maire, 2009). Although poorly studied in the academia, alteration corridors are of high interest for water resources investigations, as in the northern plateaus of the *Grands Causses* of southern France (Bruxelles and Camus, 2012; Camus, 2019). Indeed, these features are expected to play a significant role in favouring groundwater flow (Dandurand *et al.*, 2014; Malcles *et al.*, 2020; Vernant *et al.*, 2022). However, the spatial distribution and impact of alteration corridors on the functioning and evolution of karstic reservoirs remain poorly constrained and understood.

This study aims at providing a geological description of the nature, geometry and evolution of alteration corridors, in order to analyse their impact on the present-day groundwater flow path. This analytical study is based on outcrops and caves of the southern border of the Larzac Causse, which provides excellent exposures and well-developed cave networks. We developed a methodology using a set of remote sensing data, allowing us to identify and to map alteration corridors at the surface, based on several morphological criteria. This approach correlates alteration corridors observed at the surface, in scarps, and in underground caves, and it provides a 3D vision of their geometry and spatial distribution at the scale of a karstified massif. Mapping of alteration corridors produces quantitative data that are statistically analysed in order to infer their 3D geometry and spatial distribution. Subsequently, we analyse their evolving relationship with groundwater flow, over geological time-scale. Our integrated geological, geomorphological and speleological approaches allowed us to identify all the successive phases of karstification and their impact on the geometry of the karstic reservoir. A particular focus was placed on the impact of pocket valley regressive erosion on the organisation of the present-day karst network and groundwater flow.

2 Geological, geomorphological and hydrological settings

2.1 Geological setting

2.1.1 Jurassic carbonate reservoir structure

The "*Grands Causses*" is a tabular Jurassic carbonate plateau that extends west of the Mesozoic South-East Basin of France, which is a part of the Tethyan margin (Dubois and Delfaud, 1989) (Fig. 1).

Sedimentation of the marine carbonate platform replaced the Triassic siliciclastic sedimentation, which unconformably overlies the Variscan basement (Lopez, 1992) (Fig. 2). Hettangian and Sinemurian dolomite and limestone were deposited in the internal domain of a carbonate platform (Hamon, 2004; Marza, 1995). Starting from mid-Liassic, the carbonate platform of the *Grands Causses* is separated from the basinal domain of the South-East Basin by an active NE-SW structural high known as the "*Seuil Cévenol*" (Fig. 3) (Baudrimont and Dubois, 1977; Delfaud, 1973). This structural high is characterized by stratigraphical gaps and reduced thicknesses of Liassic and Dogger deposits (Fig. 2). It is controlled by NE-trending normal faults that are parallel to the Cevennes Fault, inherited from a Variscan basement structure (Arthaud and Matte, 1975).

This study focuses on the Larzac plateau located on the southern margin of the *Grands Causses*. In this area, the 20m-thin Liassic marls and Aalenian limestones pinch out southeastwards onto the *Seuil Cévenol* (Charcosset, 2000). Bathonian limestone and secondary dolomite unconformably overly Hettangian dolomite in Saint-Pierre-de-la-Fage (Fig. 2), suggesting the end of the *Seuil Cévenol* activity (Baudrimont and Dubois, 1977). Nevertheless, within the Bathonian series, successive major subaerial exposures are recognised (Charcosset *et al.*, 2000), witnessing shallow sea level at that time. In the study area, palaeokarstic features are exposed above a collapsed and brecciated interval that is approximately 10 m thick. A distinctive palaeokarstic surface is identified with pedogenic features, collapsed cavities, microcaves, and nodular horizons (Fig. 2) (Charcosset *et al.*, 2000). These emersion surfaces are sealed by the Bathonian dolomite, which is thicker above the collapsed subsurface palaeokarst (Charcosset *et al.*, 2000). The karstic features related to Bathonian emersion episodes can be distinguished from later karstic features, which are the primary focus of this paper.

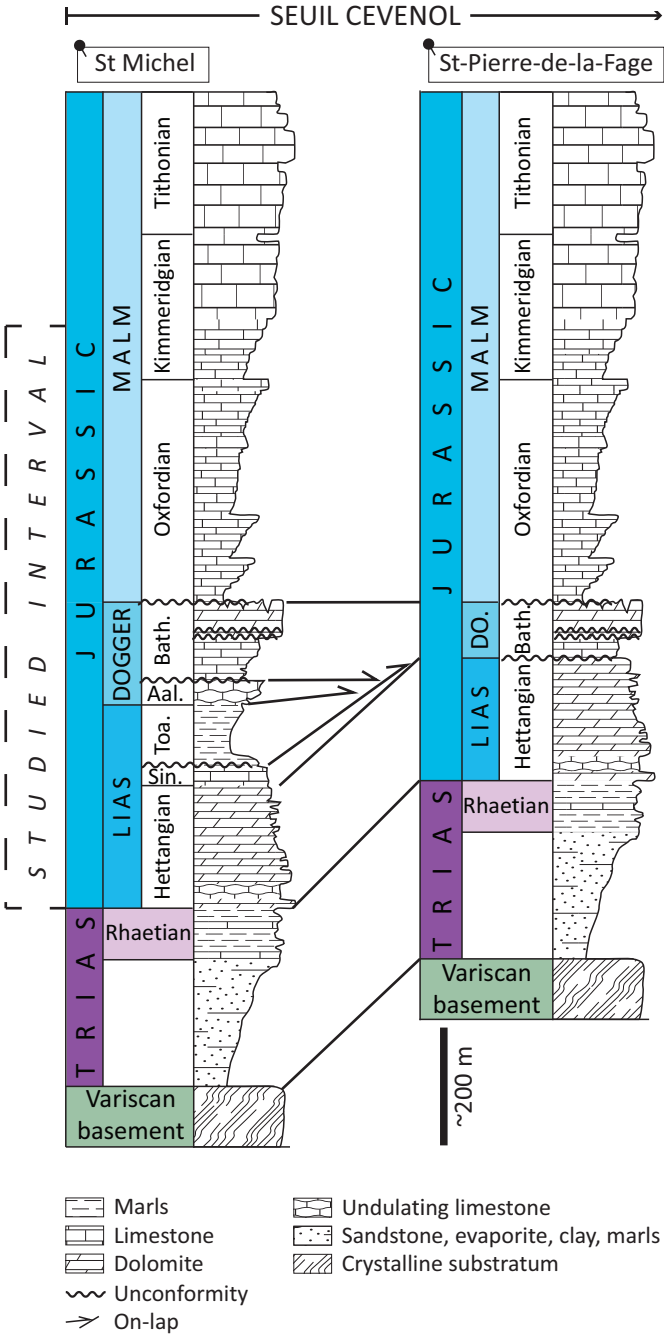

Fig. 2. Lithostratigraphic column of the southern Larzac (synthesised from Baudrimont and Dubois, 1989; Delfaud, 1979; Charcosset, 2000). Location in Fig. 3. The Seuil Cévenol is characterised by reduced thicknesses in the Grands Causses basin, which evolve in a non-depositional interval in St-Pierre-de-la-Fage by pinching-out of Sinemurian to Aalenian series. As a result, the Toarcian marly seal unit disappears towards the Seuil Cévenol leading to a unique reservoir unit constituted by Lias, Dogger and Malm carbonates.

The Malm carbonate sedimentation started with the Upper Oxfordian unconformable deposition of open-sea carbonate, followed by the development of a thick reef barrier (Séranne range, Fig. 3) on the *Seuil Cévenol* structural high during the Kimmeridgian and Tithonian (Baudrimont and Dubois, 1977).

2.1.2 Post-Jurassic evolution: from carbonate reservoir to karstic reservoir

It was classically acknowledged that the stratigraphic record of the *Grands Causses* ended with Late Jurassic limestones (Baudrimont and Dubois, 1977). However, very thin and discontinuous residual Cretaceous and Cenozoic sedimentary formations were identified (Alabouvette *et al.*, 1984, 1988; Bruxelles, 2001; Camus, 2003), which led to the interpretation of a complex succession of uplift, erosion and deposition (Séranne *et al.*, 2002) (Fig. 2). Apatite fission tracks analysis on the Variscan basement surrounding the *Grands Causses* indicate late-Lower Cretaceous kilometre-scale denudation, following kilometre-scale subsidence and sedimentation of Lower Cretaceous marine series on the *Grands Causses* (Barbarand *et al.*, 2001; Peyaud *et al.*, 2005; Séranne *et al.*, 2002).

To the southeast of the study area, in Languedoc and the South-East Basin, the marine sedimentary record continues through the early Lower Cretaceous but is interrupted by a major erosional surface (Combes, 1990). It is characterised by the deposition of bauxite in karsts that developed within the underlying limestone (Fig. 3A). This regional kilometre-scale denudation is attributed to the Durancian Isthmus uplift (Masse and Philip, 1976), which affected southern France between the Montagne-Noire and Esterel Variscan basement highs (Fig. 1) and extended across the southern *Grands Causses*, during late-Lower Cretaceous (Marchand *et al.*, 2021, and references herein).

On the southern *Grands Causse*s, marine sedimentation resumed from Turonian to Coniacian (Alabouvette *et al.*, 1988; Bruxelles, 2001). It onlaps the low-relief erosional surface with a thickness exceeding 100 m (Bruxelles, 2001). In some areas, this late Cretaceous calcareous grainstone is ferruginous and associated with corroded quartz pebbles (Fig. 4), witnessing intense continental weathering. This marks the end of marine sedimentation by Maastrichtian time on the southern Causses (Ambert *et al.*, 1978).

Laminated sedimentary-fill of palaeokarst in the Jurassic near Ganges, north of St-Martin-de-Londres and north of the study area (Fig. 3A), have yielded marine Paleocene micro- and nannofossils (Combes *et al.*, 2007; Husson *et al.*, 2012). This indicates that during the Paleocene, a marine transgression reached the *Grands Causses* (Fig. 4) and that the Jurassic carbonates were already affected by karstification, trapping sedimentary fill. Additionally, the laminated karst infillings are evidence of a hydrologically active karstic system capable of transporting sediment (Combes *et al.*, 2007; Husson *et al.*, 2012).

During the Eocene epoch, the study area was affected by the Pyrenean N-S shortening, which reactivated pre-existing faults as strike-slip or reverses faults (Arthaud and Laurent, 1995; Arthaud and Séguret, 1981; Parizot *et al.*, 2020), resulting in the deformation of the Paleocene palaeokarst (Husson *et al.*, 2012). Prior to the Oligocene rifting of the Gulf of Lion (Séranne, 1999), large endoreic depressions known as 'poljes' developed along NE-trending Pyrenean faults (Camus, 1997). The Oligocene rifting of the Gulf of Lion and the Early Miocene opening of the NW-Mediterranean Sea reorganised the watershed into a southward-flowing river network (Séranne, 1999).

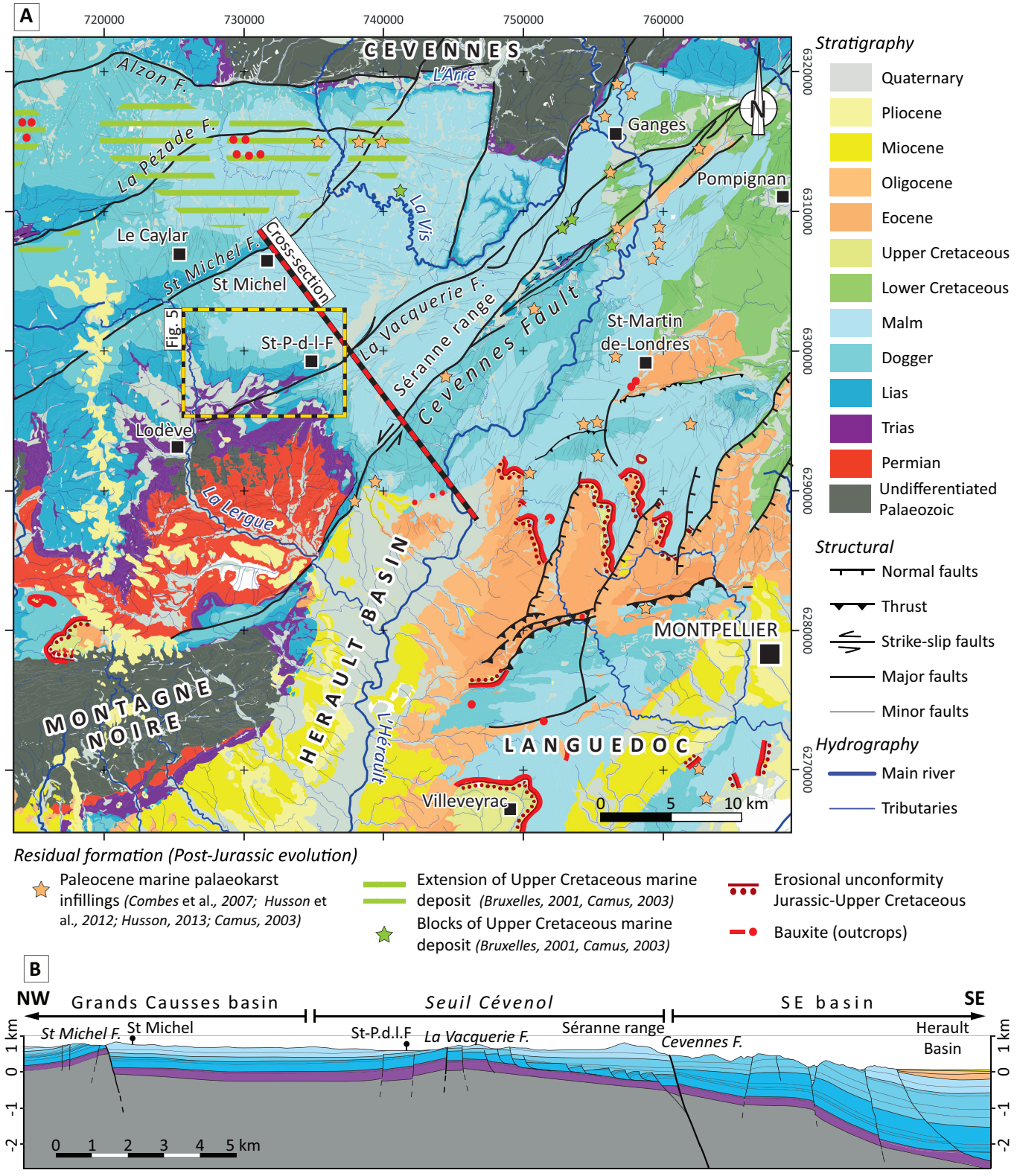

Fig. 3. A. Geological map of the Larzac Causse and the Languedoc area (location on Figure 1), synthesised from BRGM 1/50000 map. Locations of residual formations witnessing post-Jurassic evolution are overprinted (synthesised from Marchand *et al.* (2019), Bruxelles (2001), Bruxelles and Camus (2012), Camus (2003), Combes *et al.* (2007) and Husson *et al.* (2012)). B. Structural cross-section across the southern Larzac (Location on Fig. 3A) highlighting the Seuil Cévenol structural high and the reduced thicknesses of Jurassic series on the Grands Causses basin compared to the SE basin.

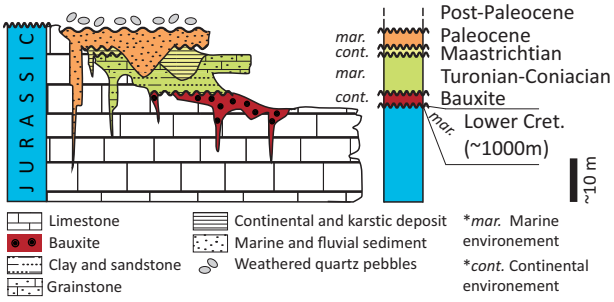

Fig. 4. Conceptual lithostratigraphic column illustrating residual formations that are witnesses of the marine and continental post-Jurassic evolution of the Grands Causses (modified from Bruxelles (2001) and Camus (2003)).

During the Late Miocene, a several-hundred-metre amplitude uplift affected the Massif Central (Séranne *et al.*, 2002), initiating the incision of canyons such as the Vis and Hérault rivers into carbonate plateaus (Fig. 3A) (Camus, 1997; Séranne *et al.*, 2002). This was followed by the Messinian Salinity Crisis and a base-level draw down, causing deep incision of the karstic networks within the carbonate massifs that belong to the Mediterranean margin watershed (Audra *et al.*, 2004). Following the sudden Mediterranean sea level rise during the Pliocene, the karstic networks located below sea level were sealed by Gilbert deltas, filling rias (Ambert *et al.*, 1998; Audra *et al.*, 2004; Clauzon *et al.*, 1990). The vertical incision of canyons was replaced by regressive lateral erosion and the development of pocket valleys (Lergue, Arre) (Séranne *et al.*, 2002). During the Quaternary, fluvial networks continued to incise their riverbeds, resulting in stepped terraces, while valleys were widened by landslides and gelifraction (Camus, 1997).

2.2 Geomorphological setting

The study area is located on the flank of a large-scale open syncline, oriented NE-SW, which can be described as a low-angle monocline that dips toward the N-NE in the study area (Fig. 5). It is bounded by the Lergue River to the west, the Vacquerie Fault to the south and east and the Saint-Maurice polje to the northeast (Fig. 5). A polje is a distinctive landform characterised by a large depression with a flat bottom and steep peripheral slopes, associated with a karstic drainage system that includes swallow holes, known as ponors (Gams, 1978). The Saint-Maurice polje develops along the Vacquerie Fault, and its bottom is covered by a semi-permeable residual formation (Camus, 1997). On the western border of the plateau, the ruiniform relief in the Bathonian dolomites reveals the weathering profile of an exhumed cryptokarst (Ambert and Ambert, 1995) (Fig. 5). Cryptokarst refers to the forms resulting from the dissolution of carbonate below a permeable cover (Ford and Williams, 2007).

The Lergue River and its tributaries are recharged by several pocket valleys and their upstream springs. These valleys are characterised by their deep, narrow and flat-bottomed profiles, ending in a steep amphitheatre-like head. They are formed through headward recessive erosion driven by a lowered base-level causing the emergence of karstic spring at the base of the carbonate massif, which is undercut by the associated underground flows (Ford and Williams, 2007; Gunn, 2004). The karstic springs are located at the bottom end of these valleys, at the interface between an impermeable substratum and a reservoir unit. The Lergue pocket valleys exhibit a dendritic pattern with multiple cirques and springs that develop in various directions, similar to those found in Slovenia (Tičar, 2015). This study focuses on the eastern pocket valleys that have cut into the southern Larzac Jurassic carbonate plateau (Fig. 5). The karstic springs associated to each pocket-valley are, from west to east, the Soubès, Avocat and Parlatges springs (Fig. 5). These pocket valley reveal entrances of four distinct cave systems within the Hettangian interval: Soubès, Gourgas, Bacou, and Banquier caves, respectively. The Banquier Cave, stands out as one of the primary cave systems of the southern Larzac, with a total length of 12.5 km.

2.3 Hydrogeological setting

The Jurassic carbonate interval is split into lower and upper aquifer units, separated by a thin Liassic marly seal unit (LM). The lower aquifer unit comprises Liassic carbonate (LC), encompassing Hettangian dolomite and Sinemurian limestone. The upper aquifer unit consists of Dogger and Malm carbonates. Although the upper aquifer is considered as a single entity, it is distinguished here as the Dogger carbonate (DC) and the Malm carbonate (MC) (Fig. 5). Below these Jurassic series, there are Triassic marls, clays and evaporites which form an impermeable substratum (S). Towards the *Seuil Cévenol* structural high, the 20 m thick Lias marls pinch out, resulting in a non-depositional gap around St-Pierre-de-la-Fage (Fig. 5) (Alabouvette *et al.*, 1988; Baudrimont and Dubois, 1977). In the area where the seal unit is absent, to the northeast of the study area, a hydraulic connection is established between the lower and upper aquifer units. Dye tracing operations indicate the following hydrological relationship (Fig. 5). Injection in the upper aquifer within Deux Zèbres and Vailhé caves supply Pégairolles spring in the lower aquifer situated approximately 3 km to the SW and 2.5 km to the SSW, respectively (Larzac Explo, 2021). This spring then directly flows into the Lergue River. Surprisingly, injection into the Perles Cave within the upper aquifer supplies Soubès spring in the lower aquifer, located 2 km to the south (Larzac Explo, 2021). A similar observation is made with the injection in the Saut du Lièvre Cave, in the upper aquifer, which supplies Avocat spring in the lower aquifer situated 7 km to the south (SpéléoClub de Lodève-Groupe Vallot, 1985). This is noticeable because the tracing fluid must cross the seal unit. Injection in the lower aquifer within the Pont Noir sinkhole supplies Avocat spring, situated 2.7 km to the west in the lower aquifer (Paloc, 1972). Both of these sinking points contribute as tributaries to the Lergue River. However, injection in the Cochon Cave, which is located only 4 km from Avocat spring, supplies both the Avocat spring (Larzac Explo, 2023) and a spring located 10 km NE, in the canyon of the Vis River (Fig. 3), which flows away from the study area (Larzac Explo, 2022).

These dye-tracing operations illustrate that recharge on the plateau is mainly hydrologically connected to the Lergue watershed. The NE area is located near the groundwater divide separating the Vis and Lergue river watersheds. Recharge in

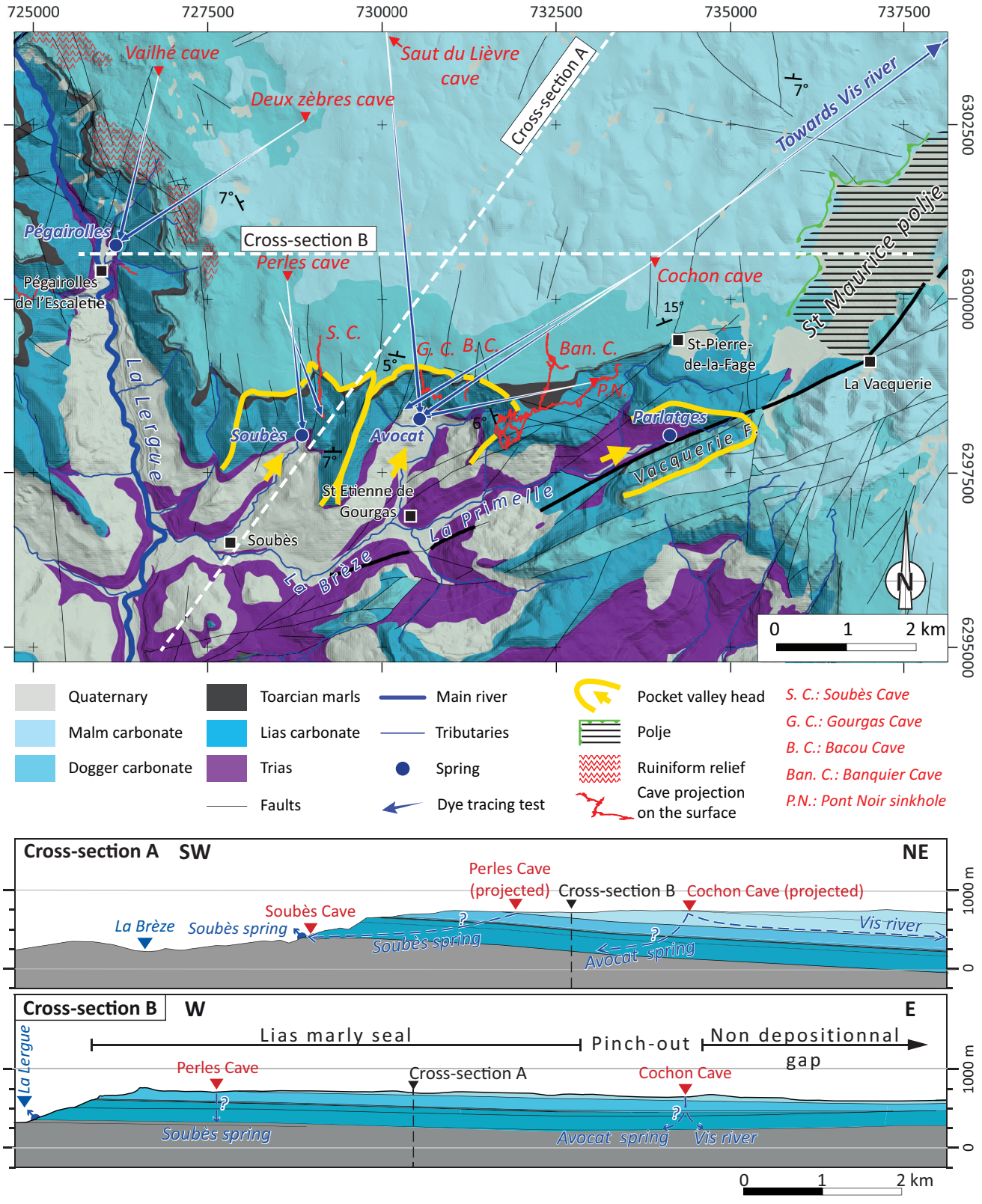

Fig. 5. Simplified geological and geomorphological map of the study area (location in Figure 3), synthesised from BRGM 1/50000 map of Le Caylar (Alabouvette *et al.*, 1988), with speleological networks projected vertically on the surface in red, compiled from the Larzac Explo Celadon database (Larzac Explo Celadon, 2023). The locations of cross-sections are indicated by white dotted lines on the map. Cross-section A reveals the plateau as a monoclinal ramp gently dipping to the North. Cross-section B highlights the pinch-out of the seal unit eastwards, resulting in a non-depositional gap near St-Pierre-de-la-Fage. Consequently, to the east, the aquifer is continuous, whereas to the west, the upper and lower aquifers are separated by a marly seal unit.

the upper aquifer is in hydrological connection with the lower aquifer pocket valleys springs with no regard for the presence of the marly seal unit. Consequently, the plateau is characterised by multiple karstic drainages, each associated with a pocket valley spring.

3 Methods

3.1 Analysis of karst reservoir organisation

In order to reconstruct the long-term evolution of the carbonate massif, we analysed geological, geomorphological, hydrogeological, and speleological data. In a first step, we constructed geological cross-sections using both the published geological map (Alabouvette *et al.*, 1988) and field measurements of bedding planes. Then, karstic and palaeo-karstic features were analysed, taking into account geology, sedimentology and geomorphology. These features were mapped on the surface and within caves. Such comprehensive mapping allowed us identifying the successive stages of karstification processes (Jouves, 2018). Additionally, we analysed the vertical profile of caves, which provides information regarding their hydrological position within the karstic system. This implies distinguishing the vadose, epiphreatic or phreatic zones, and also identifying the recharge type (regular *vs.* irregular) and the base level changes (lowering *vs.* rising) (Audra and Palmer, 2011; Jouves, 2018).

3.2 Remote sensing

This 3-dimensional approach encompasses surface remote sensing mapping over a 4 × 12 km area on the southern edge of the plateau, detailed scarp analysis, and underground investigation. We integrated sets of remote sensing data sourced from the IGN online facility (French National Geographical Institute). These data were displayed and analysed using QGIS 3.28.2 software, with the RGF93-Lambert 93 (EPSG:2154) geodetic georeferenced system.

We used Digital Elevation Model (DEM) data with a pixel resolution of 1 m in both the x and y-directions and 0.7 m in the z-direction, provided by the IGN online facility (Fig. 6A). A slope digital model was computed with QGIS software, and displayed with a black-and-white colour scale. We applied a minimum threshold of 2 degrees and a maximum of 20 degrees for visualisation. We integrated, historical (1960) and present-day aerial orthophotographs featuring pixel resolutions of 0.5 m and 0.2 m in the x and y-directions, respectively. Historical aerial orthophotographs allow to assess the persistence of landscape morphologies over time and to reveal concealed extensions or individual structures, now hidden beneath vegetation. Combining orthophotos, DEM and slope model, we highlighted 10-m scale linear dry valleys that are not associated with an upstream watershed on the surface (Fig. 6B). Although some of these structures were identified on the geological map as faults (Alabouvette *et al.*, 1988) (Fig. 6C), they do not offset the bedding. Such structures are depicted as linear furrows with a flat bottom. Where they intersect the scarp bounding the plateau, they form concave notches, extending vertically over tens of meters (Fig. 6D). The slope digital model emphasizes these morphological features by highlighting the contrast in slope between the steep edges and the flat bottom (Fig. 6E). On both present-day and ancient aerial photographs, these features appeared as grassy meadows, while the steep edges display bare bedrock and bushes (Fig. 6F). Smaller-scale karstic features, visible on aerial orthophotographs in the western part of the study area are also mapped (Fig. 11E). We then conducted statistical analyses of the orientation and spatial distribution of the identified karstic features.

3.3 Field data acquisition

Fieldwork involved measuring the orientation of bedding planes, fractures, and elongated karstic features. Additionally, we integrated speleological data including maps and speleological descriptions (Larzac Explo Celadon, 2023). Orthophotograph survey, using a drone, allowed us generating a photogrammetric model of the vertical outcrop within the upper section of the bounding scarp, from which we extracted an E-W vertical photomosaic (Fig. 7A), featuring a pixel resolution of 0.05 m in both horizontal and vertical directions. Such high-resolution photomosaic enabled us to accurately interpret the karstic features on the scarp bounding the plateau, which provides a vertical cross-section of the carbonate massif.

4 Results

4.1 Karstic features on the surface

Dry valleys are approximately 10 m wide and extend for several hundred metres across the plateau, where they predominantly align in an N-S direction. These dry valleys are correlated with sub-vertical corridors visible on the scarp, implying that they represent the surface expression of corridor structures. The dry valley floor displays specific blocks of ferruginous sandstone and microconglomerate (Fig. 7B) standing out in stark contrast to the surrounding limestones.

Observation of the vertical scarp of Bathonian limestones and dolomite (Charcosset *et al.*, 2000) reveals that these sub-vertical corridors intersect the bedding planes without any offset (Fig. 7A). They extend throughout the height of the scarp, even crossing through the early stage Bathonian karstic, 10-m thick, brecciated interval, described by Charcosset and others (2000). Further down the slope, these corridors transition into thalwegs within the Sinemurian and Hettangian limestone and dolomite layers. The sharp vertical edges of the corridors separate a brecciated and collapsed centre from the adjacent undeformed and unaltered limestone beds. These corridors are composed of crackle breccia (Loucks, 2007) (Fig. 7C) with blocks ranging from 0,1 to 3 m in size, evolving into mosaic and chaotic breccia, as the degree of blocks movement and rotation increases. These blocks can be either cemented by chemical or sedimentary deposits, such as lithified ochre to orange colour, carbonate mudstone and siltstone (Fig. 7E) that exhibit cross-bedding and finely laminated bedding.

Similar sediments are also present in tubular karstic conduits, ranging from 0.1 to 1-m-scale, affecting the carbonate massif, outside the corridors (Fig. 7D). These karstic conduits are located both above and below the

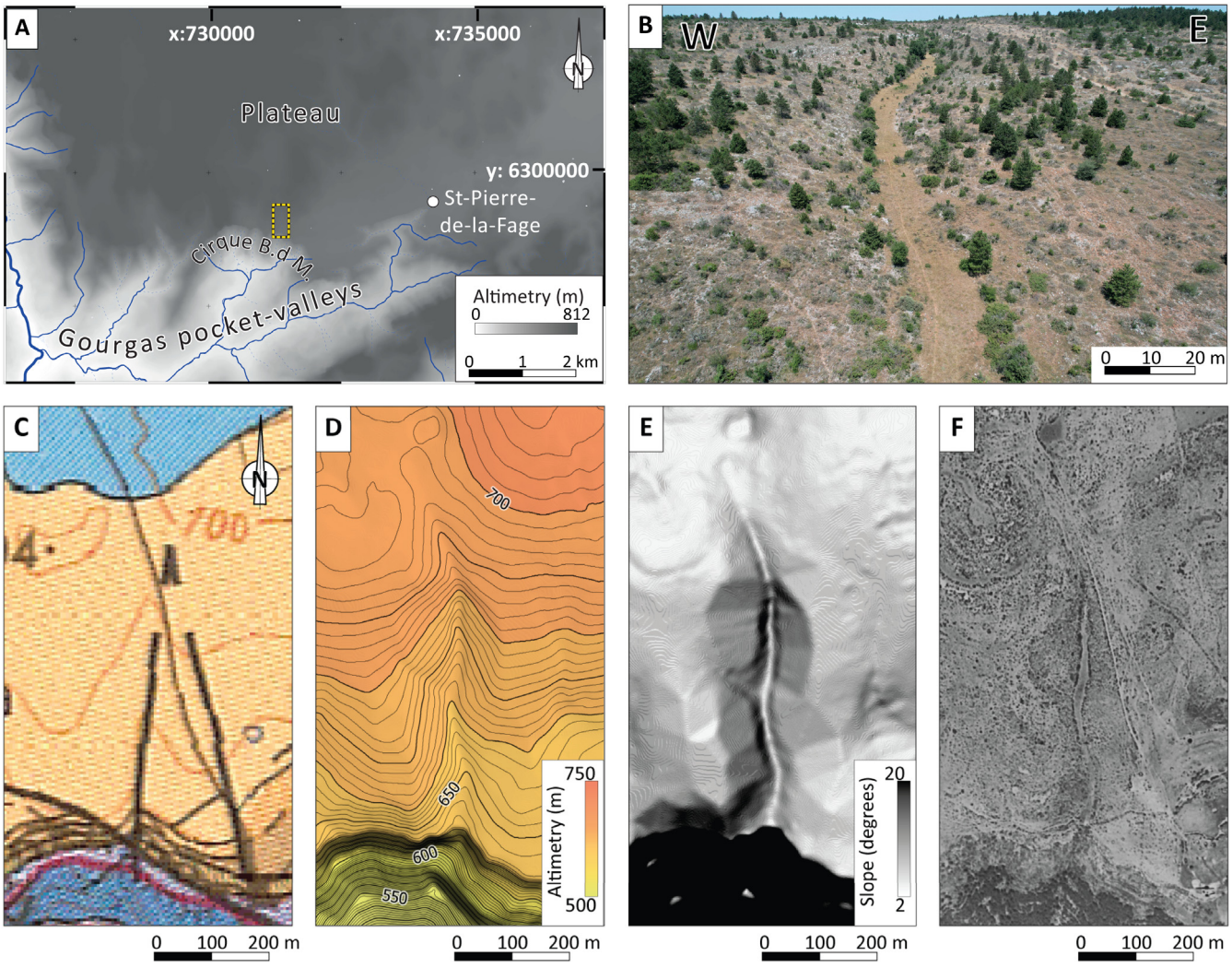

Fig. 6. A. Digital Elevation Model (DEM) of the study area (location shown in Figure 5) with a 1-m pixel resolution, sourced from the IGN online facility. B to F. Various views of the same alteration corridor identified on the field, which were used to establish a set of morphological criteria (location shown in A). B. Drone oblique view of a linear dry valley not associated with an upstream watershed on the surface. C. On the geological map (Alabouvette *et al.*, 1988), this same feature is interpreted as a fault, although it does not offset beddings. D. On the DEM, it can be described as a linear furrow, and where it intersects with the scarp, it forms a concave notch. E. The slope model highlights the contrast between the steep scarp and the flat bottom of the dry valley. F. In historical aerial photographs, it appears as a grassy meadow, while the steep edges display visible bedrock and bushes.

Bathonian emersion surface described by Charcosset and others (2000), suggesting a formation age younger than the Bathonian. These palaeo-conduits intersect the strata and partially utilise sub-horizontal bedding planes. The laminated and rhythmic infill within these conduits suggests sediment transport and deposition by hydrodynamic flow, capable of transporting and depositing sediment through open karstic discontinuities. Their position in the upper section of the escarpment indicates that this hydrological activity occurred before the formation of pocket valleys.

Lower down within the pocket valley, erosion has partially excavated a corridor in a steep-sided thalweg (Fig. 8A). This corridor displays a stepped, flat-bottom structure controlled by the sub-horizontal bedding of the Hettangian dolomite, while the edges consist of massive, unaltered dolomite. The thalweg exhibits intense vertical jointing, forming a crackle breccia without offsets (Loucks, 2007) (Fig. 8B). The walls of the thalweg correspond to a set of sub-vertical fractures oriented around N170 and N100. These fractures govern the regressive erosion by dismantling blocks (Fig. 8C). Such corridor morphology is consistent with the ones observed across the scarp.

Within a vertically elongated hollow structure at the bottom end of the thalweg, we observe zones of competent dolomite embedded in soft dolomitic sand, preserving the initial rock bedding (Fig. 8D). A similar observation is made within a horizontal stratiform structure. These features are indicators of alteration due to the ghost-rock karstification

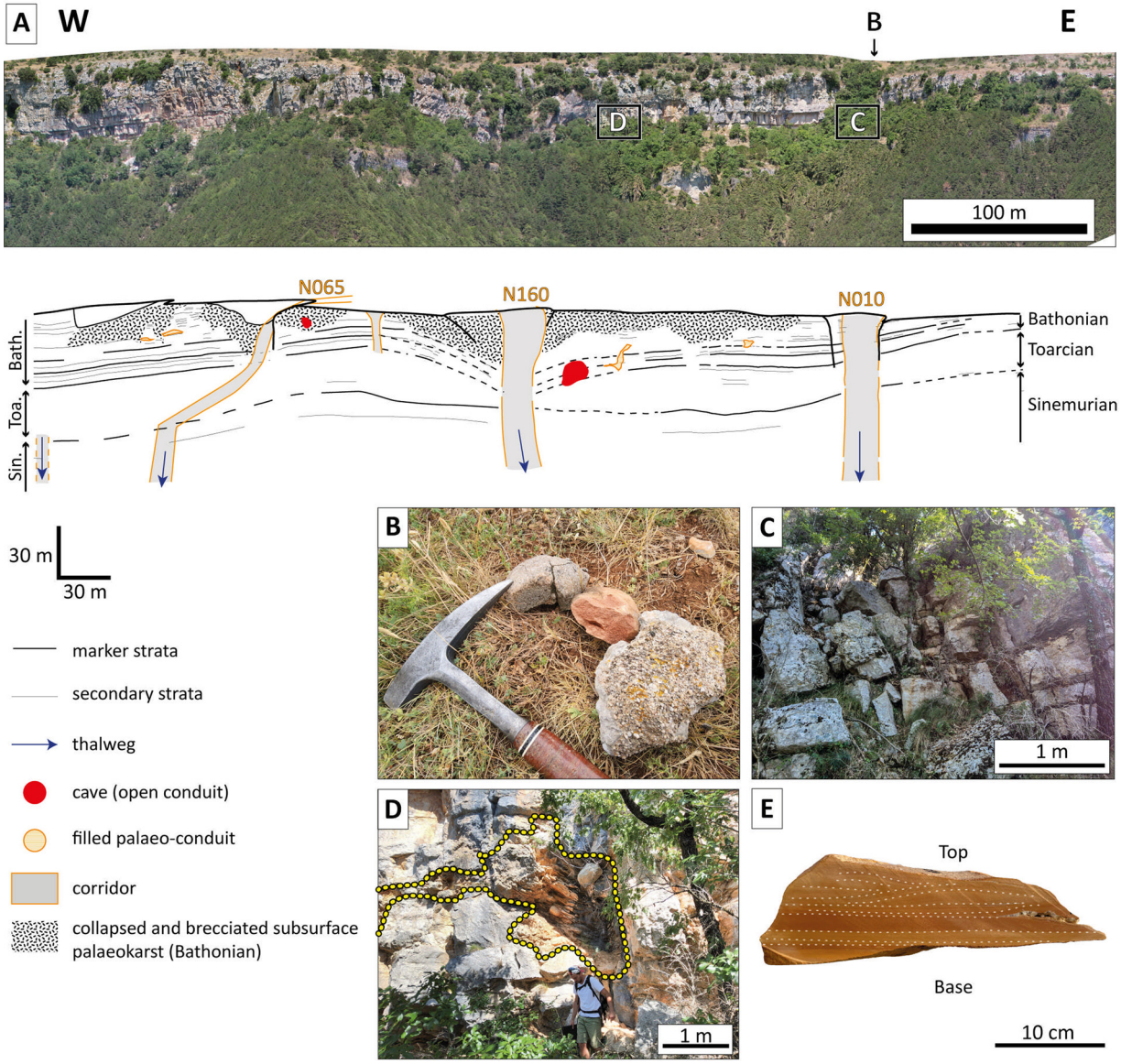

Fig. 7. A. Photomosaic extracted from the orthophotograph survey conducted on the upper scarp of the Cirque du Bout du Monde (location shown in Figure 6 as Cirque B.d.M.) using a drone. The easternmost vertical corridor aligns vertically with the flat-bottom valley observed on the surface (illustrated in Figure 6), implying that in cross-section the dry valley presents a corridor structure. The stratigraphy is based on Charcosset *et al.* (2000). Vertical corridors extend across the entire scarp and change into thalweg in the forested slope without offsetting beddings. Note that the western corridor, vertical and oriented N065, is obliquely cut by the scarp. B. Ferruginous sandstone and microconglomerate blocks found on the surface within the dry valley (shown in Figure 6). C. The corridor's centre consists of breccia with divided blocks that keep their initial positions or have collapsed. D. Metre-scale palaeo-conduit (yellow dotted line) filled with lithified laminated sediment. This palaeo-conduit develops within a vertical discontinuity and a bedding plane. E. Laminated lithified sediment found in corridors centre between blocks and within palaeo-conduits. These finely laminated siltstones exhibit cross-bedding, indicating sediment deposition by hydrodynamic processes.

process (Dubois *et al.*, 2014; Vergari and Quinif, 1997). Notably, this corridor aligns with the Soubès cave (Fig. 8A), suggesting that the latter may represent an underground extension of this ghost-rock corridor.

4.2 Underground karstic features

The Banquier Cave stands as one of the largest known cave system in southern Larzac, extending over 12.6 km (Aussenac *et al.*, 2022). It primarily develops parallel to the base of Hettangian limestone, which dips 5°N (Fig. 9). This interval is characterised by the '*Parlatges facies*' (Lopez, 1992), which consists of undulating mudstone underlined by marly bedding planes. The Northern gallery (Fig. 9), reaches up the conformably overlying Sinemurian limestones. During high-flow events, the Lower Entrance becomes an overflow spring. The Western and Eastern galleries lie below the elevation of this overflow spring, at 425 m above sea level. The Eastern gallery has been explored by cave-diving (Camplo and Vasseur, 2023), revealing its composition of 3 submerged segments connecting 2 emerged passages (Aussenac *et al.*, 2022). The lowest point in this gallery descends to 371 m above sea level, which is 54 m below the Lower Entrance.

The speleological survey of the Western gallery (Fig. 10A), revealed 3 distinct morphological features; (1) corridor galleries, (2) tube galleries and (3) stratiform dissolution.

Corridor galleries are planar, tens of meters high and several metres wide. Collapsed blocks, visible on the floor and ceiling, are stuck between the walls, obscuring the complete vertical extension (Fig. 10B). Walls are made of unaltered and undeformed rock and the stratification plane is consistent across the gallery, without offset or dip change. These vertical structures predominantly align in a N-S direction.

Tube galleries are metre-sized tubes excavated into unaltered bedrock (Fig. 10C). The walls of these galleries are marked by multiple scallops (Curl, 1966) pointing out a westward waterflow (Fig. 10A). This characteristic is also observed in the Eastern gallery explored through speleo-diving (Camplo and Vasseur, 2023). These galleries are by-passes that intersect corridor galleries, creating a network that displays looping passages (Fig. 9, blue gallery). The formation of these galleries and the associated network morphology results from water dissolution triggered by periodic high-flow events, distinctive of the epiphreatic zone (Audra, 1994; Audra and Palmer, 2011; Häuselmann, 2002).

Inter strata / stratiform dissolution features, observed in both corridors and by-pass galleries, exhibit specific parietal forms: (1) ceiling pockets, (2) differential dissolution features and (3) notches and projections, collectively referred to as 'ghost-microforms', as described by Dubois *et al.* (2022). These morphologies become visible on the walls and ceilings after the removal of residual alterite (Dubois *et al.*, 2022). Figure 11D illustrates an example of irregular walls resulting from differential dissolution, with clay-rich strata still in positive relief. In a dead-end of this chamber protected from erosion, we observe unaltered host rock with strata lamination intersected by calcite veins, transitioning into a soft rock featuring consistent laminations and calcite veins (Fig. 10E and 10F). The soft rock represents residual alterite still filling the differential dissolution feature, offering evidence of in-situ dissolution by ghost-rock karstification.

The set of morphological criteria used to identify galleries is applied to other galleries within Banquier Cave, as well as Bacou, Gourgas and Soubès caves, based on their respective speleological maps (Aussenac *et al.*, 2022; Gauffre and Gayet, 2020; Géa *et al.*, 2020). Linear galleries in the Northern and Southern galleries of Banquier Cave, Bacou, and Gourgas caves are associated with numerous blocks on the floor, as indicated on speleological maps. Soubès cave is characterised by a linear gallery with a 10-m vertical extension, also displaying blocks on the floor and ceiling (Baraille and Vasseur, 2023). These galleries are therefore classified as corridors.

These observations suggest that corridor morphology is consistent both underground and at surface. Moreover, evidence of in-situ alteration remnants is found in corridors and in inter-strata / stratiform dissolution features. Thus, we assume that corridors visible on the surface extend vertically underground, through the entire thickness of the Jurassic carbonate. The development of these corridors is influenced not only by the jointing network but also by the ghost-rock alteration process. The relationship between water flow and corridors evolution is highlighted by: i) the position of corridors relative to thalwegs, ii) the presence of epiphreatic galleries, and iii) the laminated infillings.

4.3 Orientation distribution of surface and underground corridors

Based on the distinctive morphological criteria, a total of 360 corridors were mapped within a 40 km^2 area, including 330 on the surface (Fig. 11A) and 30 underground (Fig. 10A). These corridors typically exhibit an open-angle zig-zag shape and predominantly follow an N-S direction. Notably, corridor intersections often coincide with diamond- or star-shaped dolines where each branch corresponds to a corridor. To facilitate analysis, these zig-zag-shaped corridors have been divided into rectilinear segments, defined by their centreline (Fig. 11B). In total, we mapped 993 rectilinear segments and associated them with a set of geometrical (length, azimuth) and geological (stratigraphy, lithology) parameters.

The 40 km^2 area of investigated outcrops on the plateau comprises 13 km^2 of Bathonian dolomite, 16 km^2 of Oxfordian limestone and 11 km^2 of Kimmeridgian limestone. In Oxfordian and Kimmeridgian limestone, the density of rectilinear segments is comparable, with approximately 16 and 18 segments per km^2, respectively. However, in Bathonian dolomite, the density of linear segments in corridors is higher, with approximately 28 segments per km^2. Furthermore, corridors' rectilinear segments in Oxfordian and Kimmeridgian limestones average about 140 m in length, whereas in Bathonian dolomite, they are 95 m long in average.

Analysis of the orientation data (Fig. 11C) reveals that 40% of the measured segments on the surface align with an N-S direction, gathering in N150 to N180 and N000 to N010 azimuth ranges. An additional 25% of segments show orientations ranging from N010 to N030 and N0150 to N0130. Thus, approximately 65 % of the measured segments on the surface

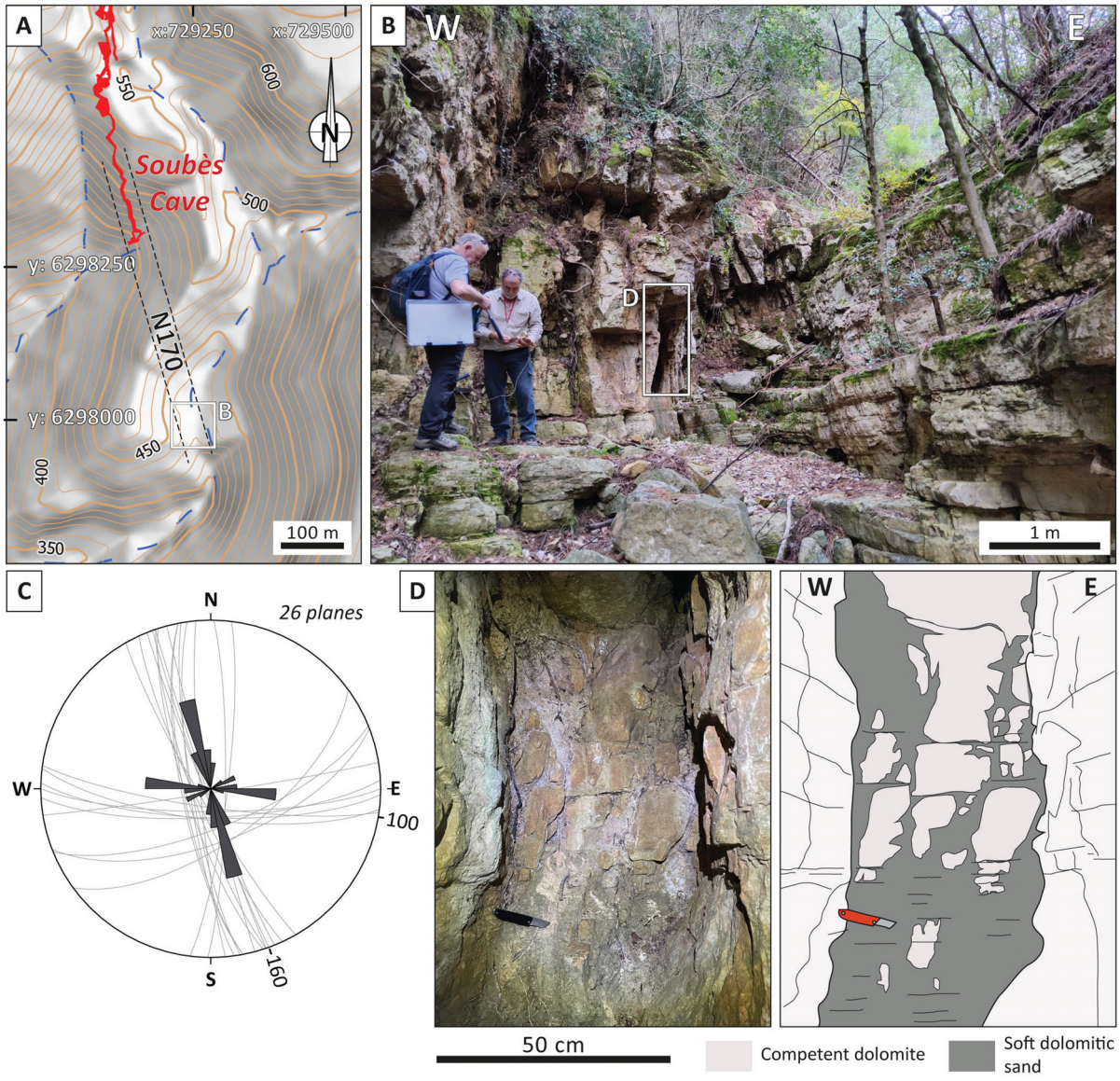

Fig. 8. A. In the Hettangian dolomite, a steep-sided thalweg with a flat bottom aligns with the Soubès Cave (location shown in Figure 5). B. Cross-section of the thalweg shows intense vertical jointing. The flat bottom is made of sub-horizontal bedding, in a ≤ 25 m^2 area. C. The rose diagram displays the orientation data of 26 fracture planes (ranging from 0,1 to 1m-scale) measured at the lower end of the thalweg. D. Within a protected elongated hollow structure (location shown in B), blocks of competent dolomite are embedded in soft dolomitic sand, preserving the initial rock bedding. The pocket knife thrust into the soft dolomite illustrates the in-situ alteration process of ghost-rock karstification.

exhibit an orientation close to N-S with a maximum around N170. The remaining segments observed on the surface are evenly distributed across other orientation categories.

Although there is limited underground measurement (62 segments) from Soubès, Bacou, Gourgas and Banquier caves, it appears that corridors display azimuth ranges from N170 to N180 and from N000 to N020 (Fig. 11D).

On the surface, the corridors typically exhibit a 100-m-scale spacing (Fig. 11A), except for the westernmost border of the plateau, where a ruiniform relief develops in Bathonian dolomite. In this specific area, a set of corridors with a 5 to 10 m spacing is revealed between the larger scale corridors with a 100-m scale spacing (Fig. 11E). These corridors display two orthogonal directions, N070 and N160 (Fig. 11F), which corresponds to the fracture directions measured on the plateau by Barthélémy *et al.* (1996). The corridor 10 m-spacing pattern in the ruiniform relief is comparable to the one observed in Banquier Cave. Larger scale corridors seem to navigate through these orthogonal fractures, with open angle zig-zag shape individualising a structure smoothing the fracture pattern direction and forming a network with a 100-m scale spacing (Fig. 11E).

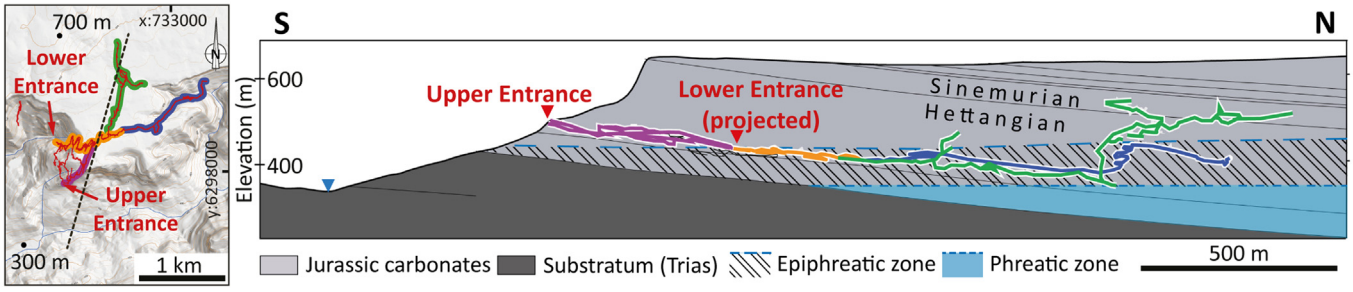

Fig. 9. Banquier Cave survey projected on the geological cross-section with colours referring to the galleries visible inset: orange corresponds to the Western gallery, blue is the Eastern gallery, green is the Northern gallery and pink is the Southern gallery. The Banquier Cave develops primarily in the Hettangian and Sinemurian carbonates. The Eastern and Western galleries are situated below the Lower Entrance height and develop parallel to Hettangian dolomite. These galleries present morphologies characteristic of the epiphreatic zone.

5 Interpretation

5.1 The structure, nature and formation of the karstic reservoir prior to pocket valley incision

Corridors affecting the 3D volume of the carbonate massif result from a post-depositional process. Such pervasive structure suggests an initial jointing network formed under tectonic stress. North-east of the study area, in similar geological setting, an orthogonal jointing pattern displaying N070 and N160 directions affects the Jurassic massif (Barthélémy *et al.*, 1996), which may represent the original jointing pattern of the whole carbonate massif, resulting from a regional palaeo-stress state. The presence of ghost-rock residual alterite within the corridors and in the Banquier Cave provides evidence of in-situ dissolution within the carbonate massif. Such dissolution occurred below the piezometric level, in a low hydrodynamic energy environment, where some chemical energy was available to dissolve the bedrock (Fig. 12A) (Dubois *et al.*, 2014). According to these authors, dissolution expands *via* diffusion from the most permeable zones within the rock, *e.g.*, the open fracture network (Fig. 12B). Ongoing dissolution continues to shape and extend the geometry of the karstic reservoir, resulting in zones of residual alterite within the core of these dissolution zones (Fig. 12C).

The centre of the corridor contains crackle breccia and collapse blocks, commonly associated with either the collapse of palaeocaves (Loucks, 2007) or with the dissolution of underlying evaporite (Friedman, 1997). Here, the formation of dissolution-collapse breccia is linked to the removal and compaction of the residual alterite that surrounds the remaining blocks. As the base-level drops, compaction of the soft residual alterite creates voids above, that facilitate groundwater circulation (Bruxelles *et al.*, 2009; Quinif, 2017). This hydraulic gradient caused by the base-level drop initiates water circulation along preferential flow paths, connecting the most favourably oriented ghost-rock features and discontinuities, thereby developing a karstic drainage system (Fig. 12D). Continued water circulation further enhances brecciation through dissolution and increases transmissivity while widening the flow path through chemical and/or mechanical erosion (Fig. 12E). These 'dissolution-collapse breccia corridors' can be viewed as an evolution of the initial ghost-rock corridors influenced by fluid-flow. The resulting drainage system can transport sediment, as evidenced by laminated sediments filling the cavities (*e.g.*, Husson *et al.*, 2012) (Fig. 12F). In the study area, sediment infill may include siliceous clasts and clay (Fig 7B), indicating an allochthonous source in addition to the local residual alterite. Consequently, the drainage system is consistent with the direction of fluid flow between an entry and an exit point.

Before incision of the pocket valley, the structure of the karstic reservoir consisted of 10-m-wide dissolution-collapse breccia corridors organised in a N-S drainage system. Furthermore, the carbonate massif contained ghost-rock features (corridors, stratiform features) that retained their alterite and developed along the initial jointing pattern. In the 3D volume, dissolution-collapse breccia corridors may join ghost-rock corridors, although some ghost-rock corridors may also remain isolated. Dissolution-collapse breccia corridors contain porous and permeable materials that facilitate fluid circulation and storage. Their vertically elongated structure allows fluid circulation from the upper to the lower aquifer, initially separated by a marly seal unit. It is suggested here that, where the Toarcian marly seal unit is present, infiltration towards the lower aquifer occurs through dissolution-collapse breccia corridors.

5.2 Speleogenesis related to pocket valley incision

5.2.1 Gravitational flow evacuation process

The Soubès, Gourgas and Bacou caves along with the Northern and Southern galleries of the Banquier Cave, include sets of N-S-oriented corridors that affect the Hettangian and Sinemurian series. These caves, situated above the current piezometric level, exhibit collapsed blocks, stuck between the corridor walls, indicating that chambers and galleries were created by the central collapse of the corridors. This implies that the residual alterite within the corridors has been removed by gravitational flow (Bruxelles *et al.*, 2009; Dubois *et al.*, 2014; Quinif *et al.*, 2014). This process of alterite removal is directly linked to the incision of pocket valleys, which led to a lowering of the base level down to the base of the Lower aquifer. Under these new hydraulic conditions, the ghost-rock corridors within the lower aquifer were emptied, resulting in the formation of voids that expose the initial ghost-rock pattern.

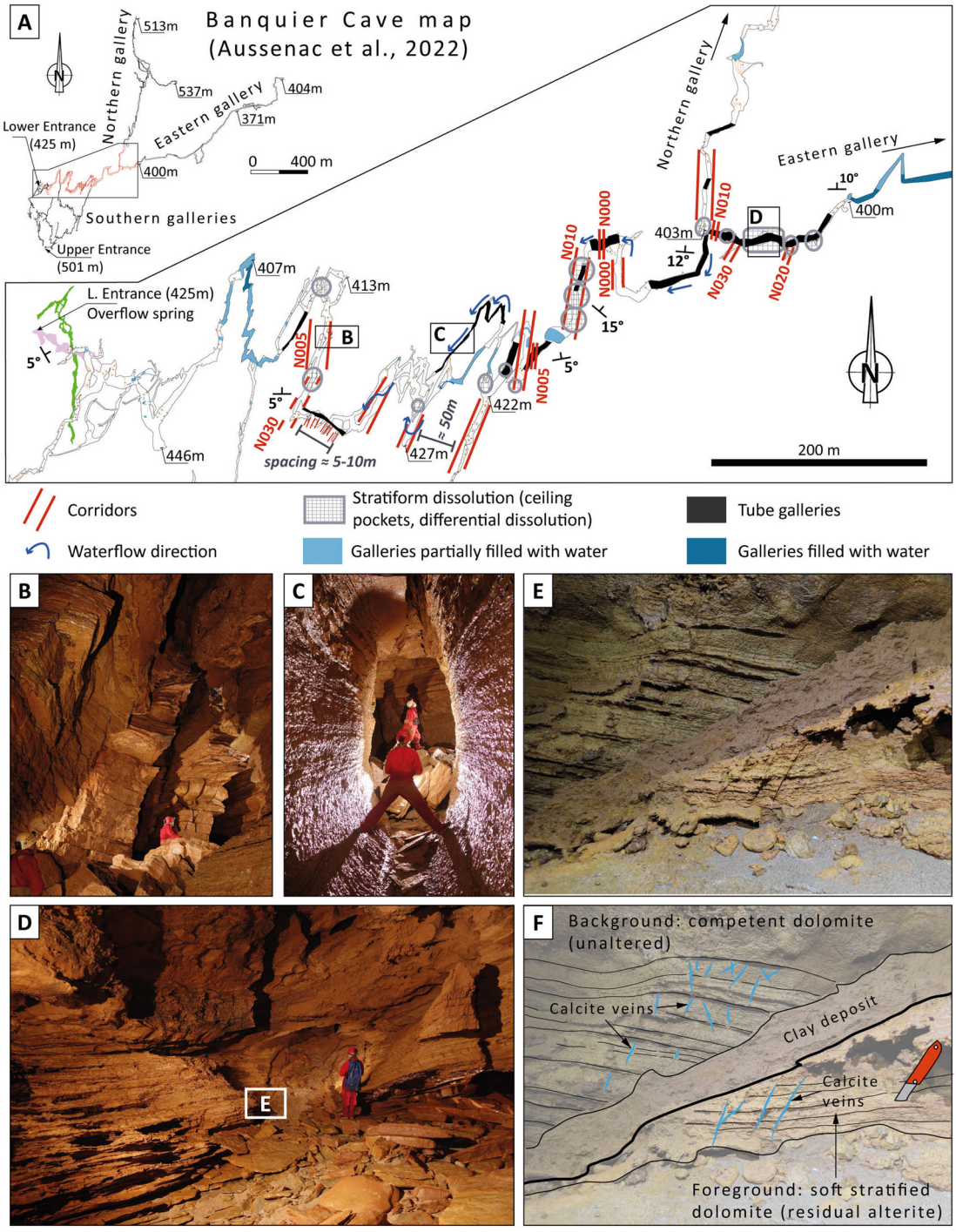

Fig. 10. A. Speleological map of the Banquier Cave adapted from Aussenac *et al.* (2022). The galleries analysed by the authors are highlighted in red on the inset map. Corridor galleries are mainly oriented N-S, and tube galleries intersect corridors. Several indicators of stratiform dissolution are identified throughout the Western gallery. B. Corridor galleries are tens of m high, with collapsed blocks on the floor and ceiling. The stratification plane is consistent across the gallery. C. Tube galleries are m-sized, and walls are marked by multiple scallops indicating a westward water flow. D. Inter-strata / stratiform dissolution is expressed by irregular walls resulting from differential dissolution, with clay-rich strata still in positive relief. E and F. Unaltered host-rock with strata lamination intersected by calcite veins transitioning into a soft rock featuring consistent lamination and calcite veins. Pocket-knife thrust into the ghost-rock residual alterite for scale. (B to D photos credit to J. Y. Bigot)

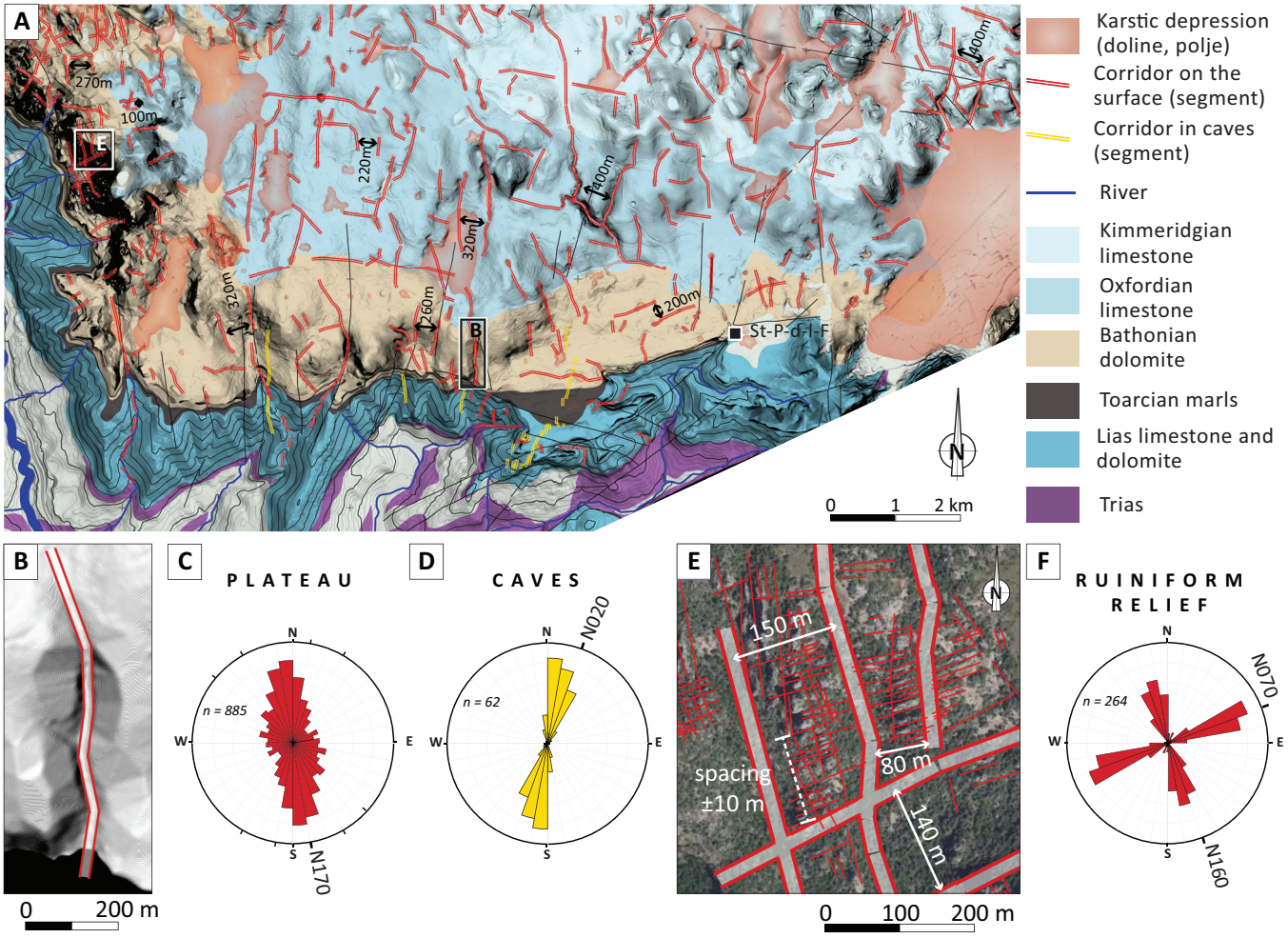

Fig. 11. A. Corridors are mapped across a 40km^2 surface on the plateau (location shown in Figure 5). To facilitate the visualisation of corridors, the slope digital model overlies the DEM on the plateau area, and contour lines are displayed in the slope. On the plateau, corridors display a 100-m scale spacing. B. Corridors are divided into a series of linear segments defined by their centreline. Corridors express a zig-zag shape and cross-cut each other. C. Approximately 65% of the measured segments on the surface display a N-S direction, with a range of 80° centred around N170. D. Underground corridors are oriented in a N-S direction and are spaced approximately 10 m apart. E. The ruiniform relief zone, in the west of the analysed area, displays corridors with a 10-m scale spacing, set between larger-scale corridors corresponding to the one mapped on the plateau. F. This set of high-frequency corridors follows two orthogonal directions, that are similar to the fracture pattern measured by Barthélémy *et al.* (1996) on the Larzac plateau.

5.2.2 Flooding/dewatering evacuation process

In the Banquier Cave, both the Eastern and Western galleries consist of corridors and stratiform ghost-rock features, intersected by tube galleries formed through groundwater flow dissolution in the epiphreatic zone (Audra, 1994; Audra and Palmer, 2011; Häuselmann, 2002). The epiphreatic speleogenesis is associated with irregular discharge and can be related with concentrated runoff into surface dolines. Residual alterite located in the epiphreatic zone are evacuated by flooding/dewatering of galleries in the cave system during periodic high-flow events (Dandurand et al., 2014).The presence of scallops on the walls of the tube galleries indicates the direction of the water flow (Curl, 1966) towards the overflow spring, situated at the westernmost part of the cave network. Notably, these Western and Eastern galleries lie beneath the temporary overflow spring, marked as the Lower Entrance at an elevation of 425m (Fig. 9). The alterite evacuation occurs in a regressive erosion dynamics (*e.g.*, Malcles et al., 2020; Quinif and Bruxelles, 2011) under powerful water flows (Dandurand et al., 2019). Tube galleries utilise and connect pre-existing discontinuities, including stratiform ghost-rock dissolution, ghost-rock corridors and bedding planes, that best fit with the orientation of the hydraulic gradient. The orientation of this gradient is controlled by the position of the pocket valley spring to the southwest. The presence of remaining residual alterite in dead-ends of galleries (Fig. 10E) implies that all the dissolution

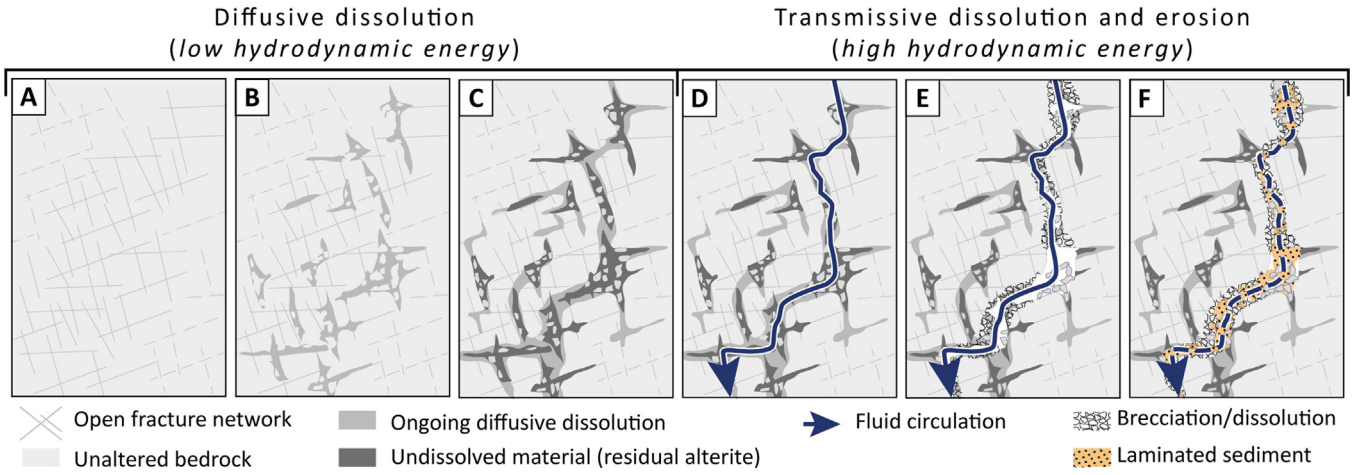

Fig. 12. Conceptual model, applicable in both cross-section and plan views, illustrating the process of ghost-rock karstification leading to the formation of a corridor network. A to C. Ghost-rock karstification occurs when the bedrock is located in the deep phreatic zone with low hydrodynamic energy. Dissolution propagates by diffusion from the most permeable zones in the rock volume (open fracture, bedding plane, permeable lithology); leaving a mesh of undissolved materials in the centre of the dissolution features. D to F. With increasing hydrodynamic energy, caused by a base-level drop, fluid circulation is introduced, controlled by a hydraulic gradient. This fluid follows preferred pathways along pre-existing discontinuities, such as ghost-rock features, and connects them while evacuating the undissolved soft material. As the fluid flows, the pathway enlarges due to dissolution and brecciation, the drainage system organises itself and it may allow for sediment transport and deposition.

features were initially filled with this material. The removal of this alterite was accomplished during high-flow events triggered by concentrated runoff on the surface.

5.3 The influence of regressive erosion in pocket valleys on the organisation of the karstic reservoir and drainage system

Pocket valley incision was initiated after the development of the Saint-Maurice polje on the plateau and the incision of the Vis River canyon in the Late Miocene (Camus, 1997; Séranne *et al.*, 2002). Consequently, before the pocket valley incision along the southern border of the study area, the hydraulic gradient was directed northwards, towards springs in the Vis River. The karstic reservoir consists of i) ghost-rock features retaining their porous residual alterite and, ii) a network of porous and permeable vertically elongated alteration corridors organised in a N-S drainage system (Fig. 13A). The cryptokarst revealed in the ruiniform relief (Ambert and Ambert, 1995) indicates the presence of a permeable non-carbonate cover above the Jurassic carbonate (Ford and Williams, 2007). Residual elements of this allochtonous sedimentary cover are found on the surface as blocks of ferruginous sandstone and microconglomerate (Fig. 7B). Such cover allowed fluvial circulation on the plateau (Bruxelles, 2001), indicating a relatively high base-level status.

A base-level drop, down to the base of the lower aquifer, initiated the pocket valley incision from the west of the study area (Fig. 13B). Dissolution-collapse breccia corridors concentrate groundwater flow due to their enhanced petrophysical properties. Their intersection with the surface provides a preferential pathway for meteoric water to reach the water table imposed by the pocket valley spring located beneath the marly seal unit. Consequently, a pocket valley karstic spring emerges at the intersection between the pocket valley scarp and the dissolution-collapse breccia corridor. The spring's position at the base of the carbonate massif leads to the immediate evacuation of the remaining residual alterite contained in the dissolution-collapse breccia corridor through gravitational flow processes. This alterite removal causes the collapse of unsupported blocks into the corridors, potentially forming caves wide enough for human exploration (Fig. 13B). Isolated ghost-rock features within unconnected carbonate volumes preserve their residual alterite (Dubois *et al.*, 2022). On the surface, the soft covering residual sedimentary formations were removed through the corridors into the karstic system (Bruxelles, 2001).

As a result, ongoing eastward regressive erosion increases the volume of carbonate massif affected by the lowered piezometric level. New karstic springs emerge at the intersection between the pocket valley scarp and dissolution-collapse breccia corridors. Caves may develop by gravitational flow evacuation of residual alterite (Fig. 13C). Each karstic spring defines a distinct pocket valley, guided by the dissolution-collapse breccia corridor. Consequently, the northward-directed regressive erosion expands the catchment of the pocket valley springs, while the hydraulic connection with the lower aquifer is still restricted to dissolution-collapse breccia corridors.

The late-stage evolution of the drainage system is characterised by the development of tube galleries between NS-oriented corridors (Fig. 13D). These intersecting tube galleries dissolve the bedrock while taking advantage of stratiform dissolution features. As a result, isolated ghost-rock features may be connected to the corridors network, and the residual alterite located in the epiphreatic zone may be evacuated by flooding/dewatering of galleries during high

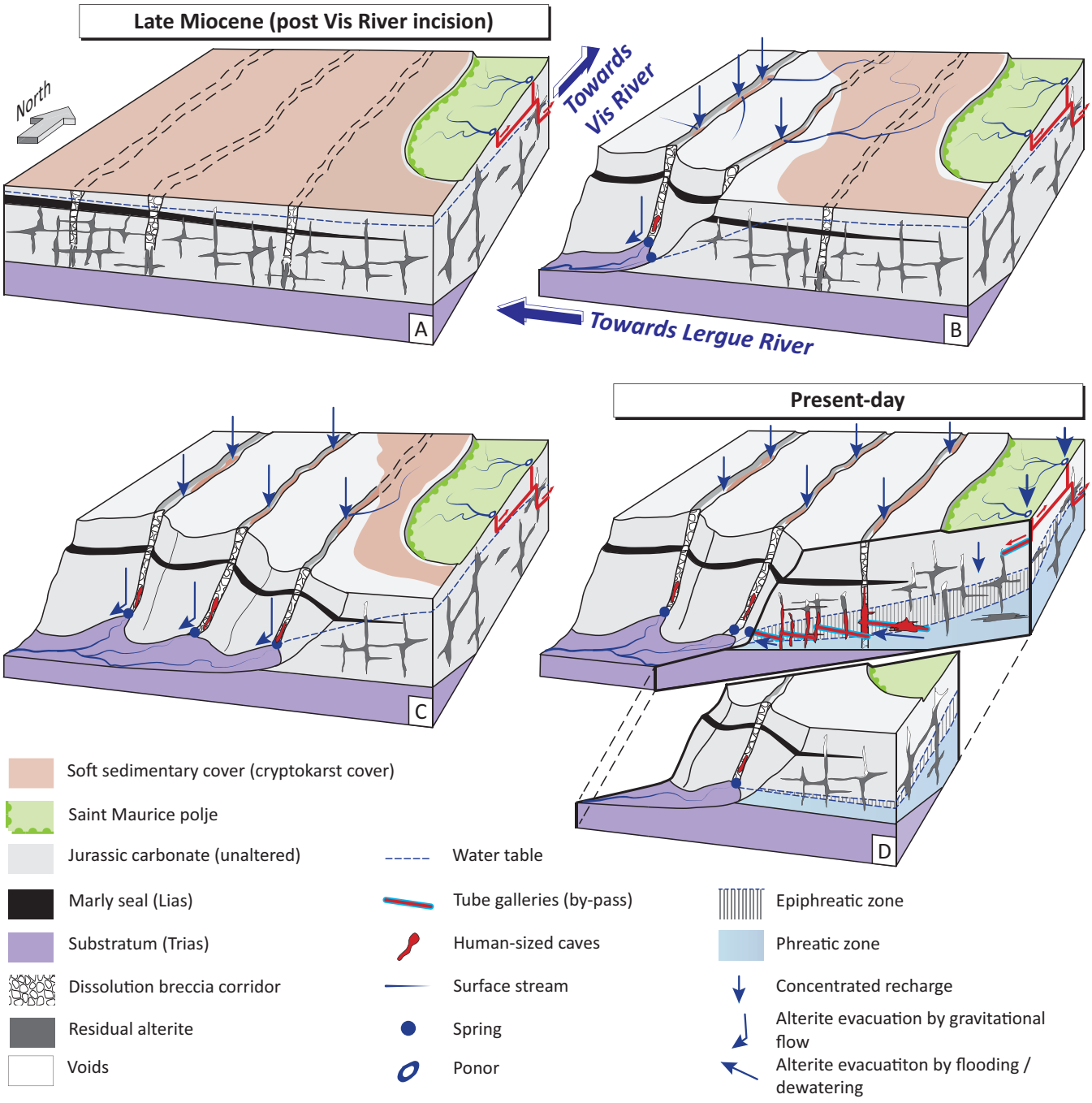

Fig. 13. A. Following the incision of the Vis River canyon, the hydraulic gradient and associated karstic system are flowing northward. The karstic reservoir consists of a network of 'dissolution-collapse breccia corridors' oriented N-S and ghost-rock associated with their residual alterite. A soft sedimentary cover lying unconformable over the carbonate allows for alluvial dynamics. B. The pocket valley initiates to the west from the Lergue River, resulting in a drop of the water table and the emergence of a karstic spring at the intersection between a corridor and the scarp. The residual alterite is rapidly evacuated and the corridor centre collapses creating caves large enough to be explored by humans. The soft covering formation is evacuated by withdrawal through the karstic system. C. Regressive erosion progresses eastward, as well as the depletion of the water table. New corridors become exposed to gravitational effects and collapse as the residual alterite is evacuated. Each karstic spring defines a pocket valley head, which propagates northwards, guided by corridors. D. In a later stage, E-W tube galleries connect isolated ghost-rock features to the corridor network. Residual alterites are evacuated by flooding/dewatering of galleries even beneath the overflow spring position during high-flow events. The combined effect of the absence of a marly seal unit and concentrated infiltration due to the St. Maurice polje allows for the development of epiphreatic speleogenesis. Regressive erosion, still propagating northward, leads to the capture of the karstic system initially flowing towards the Vis River canyon (*i.e.*, Cochon Cave).

water flow. These tube galleries indicate i) an E-W-oriented strong hydraulic gradient able to create by-passes and ii) an irregular discharge. This late-stage hydraulic modification corresponds to the eastward progression of the piezometric lowering until it reaches the hiatus of the marly seal unit. In this area, infiltrations from the plateau directly access the lower aquifer. The Saint-Maurice polje concentrates surface water towards specific swallow holes. Such concentrated infiltration in the unique aquifer unit creates favourable conditions for the development of epiphreatic speleogenesis (Audra, 1994; Audra and Palmer, 2011). Ongoing regressive erosion leads to the capture of speleological networks that were initially flowing towards the Vis River (*e.g.*, Cochon Cave).

6 Discussion

6.1 Chronology

Karstification requires an initial joint network (Quinif, 1998). The pervasive geometry of alteration corridors observed in the study area suggests that the initial joint pattern was affecting the entire thickness of the Jurassic carbonate interval, as documented by Barthélémy *et al.* (1996). In the neighbouring Villeveyrac basin (Fig. 3A), Late Jurassic carbonates are affected by a metre-scale-spacing jointing pattern, oriented N060 and N150 (Marchand, 2019), which favoured karstification and allochthonous bauxite deposition during the Albian period (Marchand *et al.*, 2021). To the north of Montpellier, Berriasian and Valanginian carbonate plateaus also exhibit similar jointing geometries (Philip *et al.*, 1978). These observations in neighbouring areas suggest that a jointing pattern affected the Jurassic and Lower Cretaceous carbonate at regional scale, before the bauxite deposition during the Albian period. In Provence, orthogonal sets of joints affecting the Upper Jurassic and the Lower Cretaceous carbonate have been interpreted as a result of an early burial stage (Lamarche *et al.*, 2012), reflecting the state of stress at the time of fracturing (Nelson, 1979). In the study area, the carbonate massif was initially buried under a kilometre-thick early Lower Cretaceous sedimentary cover, which was subsequently removed during the Aptian to Cenomanian (Barbarand *et al.*, 2001; Peyaud *et al.*, 2005). Additionally, recent U-Pb dating on normal faults calcite slickensides in the northern *Grands Causses* indicates a Barremian age (Parizot *et al.*, 2020), confirming the existence of an extensional deformation during the Lower Cretaceous, already documented in the southern Larzac (Bonijoly and Delpont, 1982). It is suggested here that the orthogonal metre-scale pervasive fracture pattern affecting the Jurassic carbonates in the study area, was formed during an early burial stage, and that it recorded the Lower Cretaceous extensional stress tensor.

During this time interval, the hydraulic gradient was very low, favouring in-situ weathering of the early Lower Cretaceous sedimentary cover (Séranne *et al.*, 2002). The weathering of the marls and limestones within the sedimentary cover promoted crypto-karstification at the top of the carbonate (Quinif, 1999). As the weathering front progressed through the carbonate massif, it provided the chemical energy required for ghost-rock karstification (Bruxelles and Camus, 2012). Therefore, in-situ diffusive dissolution, corresponding to the first stage of ghost-rock karstification, is likely to be related to the weathering of the sedimentary cover during the Aptian to Cenomanian period.

Laminated and rhythmic allochthonous lithified sediments, found in dissolution-collapse breccia corridors above and below the Bathonian palaeokarst interval, were trapped before the incision of pocket valleys, as evidenced by their position in the scarp. Similar laminated sediments trapped in palaeokarst have been documented in the surrounding areas and dated to the Paleocene (Combes *et al.*, 2007; Husson *et al.*, 2012) (Fig. 3A). Due to the similar lithofacies, stratigraphic relationships and outcrop settings, lead us to tentatively correlate the laminated sediments described in our study with these Paleocene sediment-infills. If this hypothesis is confirmed, then the first phase of residual alterite removal leading to the development of a karst forming the dissolution-collapse breccia corridor network would have occurred prior to the Paleocene. The evacuation of residual alterite implies a relative base-level drop allowing fluid flow along a hydraulic gradient. Relative base-level drop conditions can be encountered during the Durancian Isthmus uplift (Masse and Philip, 1976) that affected the southern *Grands Causses* during the late-Lower Cretaceous (Marchand *et al.*, 2021 and references herein), and during Maastrichtian to Danian period (Husson *et al.*, 2012). Further investigations in a larger area are needed to reduce the time bracket for this initial phase of the karst organisation.

Pocket valley development followed the uplift of the Larzac Causse, which occurred in late Miocene time (Séranne *et al.*, 2002) (Fig. 13A). Pocket valley regressive erosion affecting the southern border of the plateau requires that the Lergue River had already incised the downstream part of its catchment. The onset of the pocket valley dynamics therefore cannot be older than Pliocene, and so is the removal of the residual alterite from the ghost-rock corridors visible in caves.

6.2 Spatial organisation of alteration corridors

Mapping alteration corridors exhaustively in a 40km^2 area allows a quantitative analysis of their geometry that aims at identifying factors that control their spatial distribution.

In the ruiniform relief, the corridors network follows the initial fracture network, described by Barthélémy *et al.* (1996) with equal proportion of N160 and N070 structures. Meanwhile, dissolution-collapse breccia corridors observed on the surface of the plateau are mainly oriented N-S. We have shown that dissolution-collapse breccia corridors are composed of several segments exhibiting an open-angle zig-zag shape going through the orthogonal jointing pattern. These corridors existed before the onset of pocket valleys and formed a palaeokarst able to transport and trap allochthonous sediments. The geometry of these corridors is mainly driven by the phase of transmissive dissolution and erosion, which preferentially interconnects features that best fit the orientation of a hydraulic gradient. As a result, the structural control of the initial jointing pattern is partially masked and the direction of the alteration corridor is mainly driven by the orientation of a hydraulic gradient. Since dissolution-collapse breccia corridors are an evolution of ghost-rock corridors, we can assume that high-frequency ghost-rock corridors, visible in caves, are connected and coalesce during the phase of fluid flow to form the 20-m-thick dissolution-collapse breccia corridor that are visible on the surface.

In the cryptolapiaz forming the ruiniform relief, alteration corridors present a high-frequency (10-m scale spacing). This set of high-frequency corridors is located on the surface in the infiltration area of the karst. In caves, ghost-rock corridors exhibit a similar 10-m scale spacing and are located in the epiphreatic zone, which is an environment of dynamic water flows. Although corridors in the ruiniform relief and in caves present a similar high-frequency spacing, they were formed by two distinct processes, i) dissolution under a cover formation for cryptokarst and ii) in-situ diffusive dissolution by ghost-rock karstification in caves. Both these corridors are expressed in specific zones of the karst system, which are high-hydrodynamic-energy environments: the infiltration area and the epiphreatic zone. In the study area, high-frequency corridors are revealed by the hydrodynamic energy created by the base-level drop leading to the onset of pocket valleys. The frequency of corridor spacing revealed in the ruiniform relief and caves is related to their position in the karst system during the time of the evacuation of the residual alterite. Accordingly, the 100-m scale spacing of the dissolution-collapse breccia corridors, that predate the pocket valley incision, could be inherited from their position in the karst system during the first phase of alterite evacuation.

The localised occurrence of alteration corridors with a 100 m-scale spacing suggests an initial heterogeneity of the diffusive dissolution processes. According to Quinif (1998), karstification requires the combination of 3 types of energy: chemical (*i.e.*, presence of CO_2), mechanical (*i.e.*, open fracture network), and potential energy (*i.e.*, fluid flow). The presence of CO_2 being generalized in the karstic environment (Quinif, 1998) it does not play a determinant part in the morphology of karstic features (Bakalowicz, 1992). Therefore, the orientation and distribution of the dissolution corridors can be caused by either mechanical energy leading to a heterogeneous open fracture network, or potential energy causing fluid flow – although very slow –, favouring diffusive dissolution without evacuation of the undissolved material. Several examples of karstification along fracture corridors are documented in folded environments (Bagni *et al.*, 2020; Furtado *et al.*, 2022; Pontes *et al.*, 2021; Tognini and Bini, 2001), where stress tensors open a specific set of joints, which favour dissolution (Havron *et al.*, 2007). Considering a homogeneously distributed open fracture network, a weak hydraulic gradient can favour preferential diffusive dissolution along one set of joints (Camus *et al.*, 2015).

6.3 Implications for the organisation and functioning of the present-day karstic system

The pre-existing karstic network of dissolution-collapse corridors represents a significant volume of porous (up to 60%) and permeable (up to 10 Darcy) material (Dubois *et al.*, 2014), capable of storing large volumes of groundwater. The initiation of pocket valleys leads to a localised lowering of the piezometric level. Under such hydraulic conditions, the entire height of the dissolution-collapse breccia corridors is affected by gravitational removal of residual alterite (Quinif and Maire, 2009) and the formation of collapse structures (Loucks, 2007). Consequently, the section below the water table remains filled with residual alterite. The evolution of the base-level geometry within the carbonate massif depends on the northward regressive erosion of pocket-valleys, which expand the catchment to the north, eventually capturing part of the Vis River watershed. Meanwhile, due to the E-W hydraulic gradient imposed by pocket valley springs, tube galleries are formed by dissolution of the bedrock connecting alteration corridors and pre-existing dissolution features. Creation of tube galleries requires thousands to tens of thousands of years (Palmer, 2003). Once created and widened, these tube galleries provide more efficient flow paths than alteration corridors. We suggest that the kilometre-long, hundreds of metres high and tens of metres wide corridors filled with high porosity collapse-breccia provide better storage capacity with a slower, more sustained, discharge than localised linear empty galleries. Mangin (1975) described the karstic system as a combination of transmissive drains connected to an "annex system" that presents a low transmissivity but high capacity. Therefore, as suggested by Quinif *et al.* (2022), we consider that the network of alteration corridors still filled with residual alterite is an expression of such conceptual "annex system" whereas tube galleries and alteration corridors emptied of their residual alterite are transmissive drains. The investigated 40 km^2 area of the plateau reveals $>$ 50 km cumulated length of corridors about 10 m wide, that affect approximately 400 m thickness of the Jurassic carbonates. We can estimate that the envelope of alteration corridors represents 200 million m^3. These features represent a significant amount of porous and permeable media available for groundwater storage and are prone to slowly supply water to springs. We suggest that the volume of alteration corridors located below the piezometric level makes a promising prospect for water supply. However, their storage capacity and conductivity still remains to be characterised.

7 Conclusion

The karstic reservoir of the southern border of the Larzac Causse consists of i) a network of alteration corridors (dissolution-collapse breccia and ghost-rock corridors), that cross-cut the entire thickness of the Jurassic massif, and ii) volumes of isolated ghost-rock features still filled with residual alterite. These vertically elongated corridors develop regardless of the initial litho-stratigraphical layering and connect initially separated aquifers. These structures connect water infiltration on the plateau surface with the underlying aquifers and make preferential underground flow paths. Even if the effective volume still needs to be accurately quantified with an estimation of the connected porosity, this quick-look estimate highlights that the cumulated volume and internal structure of alteration corridors constitute an additional, unsuspected, underground water resource when located below the piezometric level.

The karstic reservoir results from a multi-stage evolution of a carbonate massif initially fractured, probably during Early Cretaceous. The massif was then affected by slow and long-term ghost-rock karstification by in-situ diffusive dissolution in the phreatic zone. Evacuation of the residual alterite occurred in a two-stage process. A first stage of evacuation was controlled by an N-S oriented hydraulic gradient and resulted in the development of dissolution-collapse breccia corridors, that preserved laminated sediment witnessing the functioning of an organised drainage system.

In a second stage, following the Late Miocene regional uplift, the base level dropped down to the base of the carbonate massif, initiating the regressive erosion of pocket valleys along the southern margin. The new south-directed flow reactivated the pre-existing karstic drainage system. Pocket valley springs emerged at the intersection between alteration corridors and the scarp, leading to the rapid evacuation of residual alterite. Alteration corridors enhanced and guided the regressive erosion, progressively capturing the Vis River drainage system. Later on, during the Plio-Pleistocene, tube galleries integrated isolated ghost-rock features into the drainage system and evacuated alterite in the epiphreatic zone during high-flow events. When evacuation is driven by gravitational flow, only the karstic reservoir located above the water table is mobilised. On the contrary, when evacuation is driven by flooding/dewatering of galleries in the epiphreatic zone, it indicates a hydraulic connection with the entire phreatic zone. These distinct dynamics can impact the way the karstic reservoir presently responds during low or high water periods, or during significant recharge periods.

The identification, characterisation and mapping of drainage structures on the border of the Larzac Causse provides insights into the nature, size, and connectivity of the corridors network, which represent a valuable prospect for water resources. This practical methodology can be used as a guide for future exploration and seems to be a prerequisite for hydrogeological studies in karstified carbonate massifs. Integrating these drainage structures into karstic reservoir modelling may provide a practical solution for i) quantifying the karstic reservoir volume, ii) helping decision-makers in delineating protected areas, and iii) building dynamic hydrogeological models to facilitate the management of karstic groundwater.

Acknowledgements

We are very grateful towards the cavers and cave-divers communities of the Larzac Explo and Celadon caving club which acquired and shared their cave survey data. They guided us into the Banquier Cave during their lastest exploration in July 2022. This study is part of a PhD (C.B.), with a CIFRE convention between ANRT (Association Nationale Recherche Technologie), Cenote and Géosciences Montpellier laboratory (CIFRE N°2021/1005). We thanks Jo de Waele and an anonymous reviewer for their constructive comments which improved the manuscript.

References

Alabouvette B, Arrondeau JP, Aubague M, Bodeur Y, Dubois P, Mattei J, *et al*. 1988. Feuille Le Caylar n°962. Carte géologique de la France au 1/50000. BRGM.

Alabouvette B, Azema C, Bodeur Y, Debrand-Passard S. 1984. Le Crétacé supérieur de Causses (sl.). *Géologie de la France* 1-2: 67–73.

Ambert P, Aguilar J-P., Michaux J. 1998. Évolution géodynamique messino-pliocène en Languedoc central: le paléo-réseau hydrographique de l'Orb et de l'Hérault (Sud de la France). *Geodinamica Acta* 11: 139–146.

Ambert P, Ambert M. 1995. Karstification des réseaux et encaissement des vallées au cours du Néogène et du Quaternaire dans les Grands Causses méridionaux (Larzac, Blandas). *Géologie de la France* 4: 37–50.

Ambert M, Ambert P, Coulet E, Fabre G, Guendon J-L., Nicod J, *et al*. 1978. Le Causse de Blandas. Présentation d'une carte géomorphologique au 1/25 000. *Méditerranée* 32: 3–21.

Arthaud F, Laurent P. 1995. Contraintes, déformation et déplacement dans l'avant-pays Nord-pyrénéen du Languedoc méditerranéen. *Geodinamica Acta* 8: 142–157.

Arthaud F, Matte P. 1975. Les décrochements tardi-hercyniens du sud-ouest de l'europe. Géometrie et essai de reconstitution des conditions de la déformation. *Tectonophysics* 25: 139–171.

Arthaud F, Séguret M. 1981. Les structures pyrénéennes du Languedoc et du Golfe du Lion (Sud de la France). *Bulletin de la Société Géologique de France* XXIII: 51–63.

Audra P. 1994. Karsts alpins. Genèse des grands réseaux souterrains – Exemples: Tennengebirge (Autriche), l'Ile de Crémieu, la Chartreuse et le Vercors (France). *Karstologia Mémoires* 5: 271.

Audra P, Mocochain L, Camus H, Gilli É, Clauzon G, Bigot J-Y. 2004. The effect of the Messinian Deep Stage on karst development around the Mediterranean Sea. Examples from Southern France. *Geodinamica Acta* 17: 389–400.

Audra P, Palmer AN. 2011. The pattern of caves: controls of epigenic speleogenesis. *Géomorphol: Relief Process Environ* 17: 359–378.

Audra P, Palmer AN. 2015. Research frontiers in speleogenesis. Dominant processes, hydrogeological conditions and resulting cave patterns. *Acta Carsologica* 44. DOI: 10.3986/ac.v44i3.1960. Available from http://ojs.zrc-sazu.si/carsologica/article/view/1960 (last consult: 2023/17/1)

Aussenac C, Blum L, Camplo J, Cazes G, Delaire C, Festor L, *et al*. 2022. Grotte du Banquier – Grotte de la Lauze. Plan spéléologique. Saint-Etienne-de-Gourgas, Hérault, Larzac: Larzac Explo – Celadon. Available from https://larzacexploceladon.fr/lizmap/index.php/view/media/getMedia?repository=cavitesandproject=cavitesandpath=media%2Ftopo_pdf%2FBanquier+FINAL.pdf (last consult: 2023/19/10).

Bagni FL, Bezerra FH, Balsamo F, Maia RP, Dall'Aglio M. 2020. Karst dissolution along fracture corridors in an anticline hinge, Jandaíra Formation, Brazil: Implications for reservoir quality. *Mar Pet Geol* 115: 104249.

Bakalowicz M. 1992. Géochimie des eaux et flux de matières dissoutes. In: *Karsts et évolutions climatiques: Hommage à Jean Nicod*, Pessac: Presses Universitaires de Bordeaux, pp. 61–74. Available from http://books.openedition.org/pub/10850 (last consult: 2023/12/10).

Bakalowicz M. 2005. Karst groundwater: a challenge for new resources. *Hydrogeol J* 13: 148–160.

Bakalowicz M. 2010. Karst et ressources en eau souterraine: un atout pour le développement des pays méditerranéens. *Sécheresse* 21: 319–322.

Baraille D, Vasseur F. 2023. Plongée souterraine: plongée post-siphon dans l'event de Soubes (34). YouTube. Available from https://www.youtube.com/watch?v=Z56GRwcytbg (last consult: 2023/4/12).

Barbarand J, Lucazeau F, Pagel M, Séranne M. 2001. Burial and exhumation history of the south-eastern Massif Central (France) constrained by apatite fission-track thermochronology. *Tectonophysics* 335: 275–290.

Barthélémy P, Jacquin C, Yao J, Thovert JF, Adler PM. 1996. Hierarchical structures and hydraulic properties of a fracture network in the Causse of Larzac. *J Hydrol* 187: 237–258.

Baudrimont AF, Dubois P. 1977. Un bassin mésogéen du domaine péri-alpin: le sud-est de la France. *Bull Centres Rech Explo –Prod Elf-Aquitaine* 1: 261–308.

Bonijoly D, Delpont G. 1982. Etude du bassin des causses et de la bordure Cévenole par la télédétection et la géologie structurale. Documents BRGM. 46. BRGM. 72 p.

Borghi A, Renard P, Jenni S. 2012. A pseudo-genetic stochastic model to generate karstic networks. *J Hydrol* 414-415: 516–529.

Broughton PL. 2018. Ghost-rock karstification of Devonian limestone flooring the Athabasca Oil Sands in western Canada. *Geomorphology* 318: 303–319.

Bruxelles L. 2001. Reconstitution morphologique du Larzac (Larzac central, Aveyron, France): le rôle des formations superficielles. *Karstologia* 38: 25–40.

Bruxelles L, Camus H. 2012. Etude hydrogéologique des Avant-causses du St-Affricain et du Causse Guilhaumard – Lot 2 – Géomorphologie. Rapport public. GTR/PNR/ 1212-1016. GEOTER. 88 p. Available from https://www.parc-grands-causses.fr/sites/all/files/upload/Comprendre-le-parc/champs-intervention/gestion_eau/lot_2_rapport_final.pdf (last consult: 2023/12/6).

Bruxelles L, Quinif Y, Wiénin M. 2009. How can ghost rock help in karst development? *Proceedings of the 15th International Congress of Speleology.* Kerrville, USA; pp. 814–818

Camplo J, Vasseur F. 2023. Plonge souterraine à la Grotte du Banquier (34) du S5 au S7. YouTube. Available from https://www.youtube.com/watch?v=WwSZd46NElw (last consult: 2023/9/5).

Camus H. 1997. Formation des réseaux karstiques et creusement des vallées: l'exemple du Larzac méridional (Hérault, France). *Karstologia* 29: 23–42.

Camus H. 2003. Vallée et réseaux karstiques de la bordure carbonatée sud cévenole – Relations avec la surrection, le volcanisme et les paléoclimats, Doctorat, Bordeaux: Université Michel de Montaigne – Bordeaux III, 762 p.

Camus H. 2019. Etude hydrogéologique du Causse Noir – Lot 2 – Géomorphologie. Rapport public. GTR/PNR/ 0719-1833. GEOTER. 189 p. Available from http://oai.eau-adour-garonne.fr/oai-documents/62122_TARN_AVEY_34045_2_etude_hydrogeologique_du_causse_noir_Lot_2_PNRGC_2019.pdf

Camus H, Leveneur D, Bart F. 2015. Structuration karstique des aquifères dans les massifs ophiolitiques de Nouvelle-Calédonie. *Proceedings of the Vingtièmes journées techniques du Comité Français d'Hydrogéologie de l'Association International des Hydrogéologues*. La-Roche-sur-Yon, Pays de la Loire, France. Available from https://www.mica-environnement.com/wp-content/uploads/2019/07/article-mica-environnementstructuration-karstiqueophiolites.pdf

Charcosset P. 2000. Synthèse paléogéographique et dynamique du bassin caussenard (Sud de la France) au cours du Bathonien (Jurassique moyen). *Eclogae Geologicae Helvetiae* 93: 53–64.

Charcosset P, Combes P-J., Peybernès B, Ciszak R, Lopez M. 2000. Pedogenic and karstic features at the boundaries of bathonian depositional sequences in the Grands Causses area (Southern France): Stratigraphic implications. *J Sediment Res* 70: 255–264.

Clauzon G, Suc J-P., Aguilar J-P., Ambert P, Cravatte J, Drivaliari A, *et al*. 1990. Pliocene geodynamic and climatic evolution in the French Mediterranean Region. *Paleontologia I Evolucio, Memoria Especial* 2: 132–186.

Combes P-J. 1990. Typologie, cadre géodynamique et genèse des bauxites françaises. *Geodinamica Acta* 4: 91–109.

Combes P-J., Peybernès B, Fondecave-Wallez M-J., Séranne M, Lesage J-L., Camus H. 2007. Latest-Cretaceous/Paleocene karsts with marine infillings from Languedoc (South of France); paleogeographic, hydrogeologic and geodynamic implications. *Geodinamica Acta* 20: 301–326.

COST Action 620. 2004. Vulnerability and Risk Mapping for the Protection of Carbonate (Karst Aquifers). Public report. EUR 20912. Luxembourg: Directorate-General Science, Research and Development, European Commission, Office for Official Publications of the European Communities. 297 p.

Cramer W, Guiot J, Fader M, Garrabou J, Gattuso J-P., Iglesias A, *et al*. 2018. Climate change and interconnected risks to sustainable development in the Mediterranean. *Nat Clim Change* 8: 972–980.

Curl RL. 1966. Scallops and flutes. *Transactions Cave Research Group of Great Britain* 7: 121–160.

Dandurand G, Dubois C, Maire R, Quinif Y. 2014. The Charente karst basin of the Touvre: alteration of the Jurassic series and speleogenesis by ghost-rock process. *Geologica Belgica* I: 27–32.

Dandurand G, Quinif Y, Guendon J-L., Gruneisen A. 2019. Sources vauclusiennes et fantômes de roche. *Karstologia* 74: 31–46.

De Waele J, Gutiérrez F, eds. 2022. Karst hydrogeology, geomorphology and caves. Wiley Blackwell. Chichester: John Wiley & Sons Ltd. 896p.

Delfaud J. 1973. Un élément majeur de la paléogéographie du Sud de la France au Jurassique moyen et supérieur; le Haut-fond occitan. *Bulletin de la Société Géologique de France* 15: 58–59.

Devos A, Jaillet S, Gamez P. 1999. Structures tectoniques et contraintes de cheminement des eaux dans les aquifères karstiques du barrois (Lorraine/Champagne, France). *Geodinamica Acta* 12: 249–257.

Dubois C, Quinif Y, Baele J-M., Barriquand L, Bini A, Bruxelles L, *et al*. 2014. The process of ghost-rock karstification and its role in the formation of cave systems. *Earth-Sci Rev* 131: 116–148.

Dubois C, Bini A, Quinif Y. 2022. Karst morphologies and ghostrock karstification. *Géomorphol: Relief Process Environ* 28: 13–31.

Dubois P, Delfaud J. 1989. Le bassin du Sud-Est. In: *Dynamique et méthodes d'étude des bassins sédimentaires*, (ed. Technip), Paris: Association des Sédimentologistes Français, pp. 277-297.

Ford DC, Williams PW. 1989. Karst geomorphology and hydrology. London: Unwin Hyman, 600p.

Ford D, Williams P. 2007. Karst Hydrogeology and Geomorphology. Chichester: John Wiley and Sons, 562p.

Fournillon A, Abelard S, Viseur S, Arfib B, Borgomano J. 2012. Characterization of karstic networks by automatic extraction of geometrical and topological parameters: comparison between observations and stochastic simulations. *Geol Soc London Spec Publ* 370: 247–264.

Friedman GM. 1997. Dissolution-collapse breccias and paleokarst resulting from dissolution of evaporite rocks, especially sulfates. *Carbonates Evaporites* 12: 53–63.

Furtado CPQ, Medeiros WE, Borges SV, Lopes JAG, Bezerra FHR, Lima-Filho FP, *et al*. 2022. The influence of subseismic-scale fracture interconnectivity on fluid flow in fracture corridors of the Brejões carbonate karst system, Brazil. *Mar Pet Geol* 141: 105689.

Gams I . 1978. The polje: the problem of definition. *Zeitscbrift für Geomorphologie N.F.* 22: 170–181.

Gauffre G, Gayet J-C. 2020. Aven-Event de Gourgas. Plan spéléologique. Saint-Etienne-de-Gourgas, Hérault, Larzac: Larzac Explo – Celadon. Available from https://larzacexploceladon.fr/wp-content/uploads/2020/10/Aven-Event-de-Gourgas-plan-def.jpg (last consult: 2023/19/10).

Géa P, Barrau G, Aussenac C, Blum L, Camplo J, Roux M, *et al*. 2020. Event du Bacou. Plan spéléologique. Saint-Etienne-de-Gourgas, Hérault, Larzac. Available from https://larzacexploceladon.fr/wp-content/uploads/2020/10/PLAN_BACOU2.jpg (last consult: 2023/19/10).

Goldscheider N, Drew D, eds. 2007. Methods in karst hydrogeology. International Association of Hydrogeologists. London: Taylor & Francis Group 263p.

Gunn J, ed. 2004. Encyclopedia of caves and karst science. New York: Fitzroy Dearborn, 902p.

Hamon Y. 2004. Morphologie, évolution latérale et signification géodynamique des discontinuités sédimentaires. Exemple de la marge Ouest du Bassin du Sud-Est (France), Doctorat, Montpellier: Montpellier II – Sciences et Techniques du Languedoc, 294 p.

Hartmann A, Goldscheider N, Wagener T, Lange J, Weiler M. 2014. Karst water resources in a changing world: Review of hydrological modeling approaches. *Rev Geophys* 52: 218–242.

Häuselmann P. 2002. Cave genesis and its relationship to surface processes: Investigations in the Siebenhengste region (BE, Switzerland), PhD Thesis, Freiburg: Universität Freiburg (Schweiz), 170 p.

Havron C, Vandycke S, Quinif Y. 2007. Interactivité entre tectonique méso-cénozoïque et dynamique karstique au sein des calcaires dévoniens de la région de Han-sur-Lesse (Ardennes, Belgique). *Geol Belg* 10: 93–108.

Hill CA, Polyak VJ. 2020. A karst hydrology model for the geomorphic evolution of Grand Canyon, Arizona, USA. *Earth-Sci Rev* 208: 103279.

Husson E, Camus H, Cabaret O. 2017. Les karsts de la bordure NE du Bassin aquitain: une histoire polyphasée à l'origine d'une organisation complexe. *Karstologia* 69: 9–18.

Husson E, Guillen A, Séranne M, Courrioux G, Couëffé R. 2018. 3D Geological modelling and gravity inversion of a structurally complex carbonate area: application for karstified massif localization. *Basin Res* 30: 766–782.

Husson E, Séranne M, Combes P-J., Camus H, Peybernès B, Fondecave-Wallez M-J, *et al*. 2012. Marine karstic infillings: evidence of extreme base level changes and geodynamic consequences (Paleocene of Languedoc, south of France). *Bulletin de la Société Géologique de France* 183: 425–441.

Jeannin P-Y., Artigue G, Butscher C, Chang Y, Charlier J-B., Duran L, *et al*. 2021. Karst modelling challenge 1: Results of hydrological modelling. *J Hydrol* 600: 126508.

Jourde H, Massei N, Mazzilli N, Binet S, Batiot-Guilhe C, Labat D, *et al*. 2018. SNO KARST: A French network of observatories for the multidisciplinary study of critical zone processes in karst watersheds and aquifers. *Vadose Zone J* 17: 1–18.

Jouves J. 2018. Origine, caractérisation et distribution prédictive des structures karstiques – De la karstologie aux modèles numériques 3D, Doctorat, Marseille: Aix-Marseille Université, 258 p.

Jouves J, Viseur S, Arfib B, Baudement C, Camus H, Collon P, *et al*. 2017. Speleogenesis, geometry, and topology of caves: A quantitative study of 3D karst conduits. *Geomorphology* 298: 86–106.

Kaufmann O, Deceuster J. 2014. Detection and mapping of ghost-rock features in the Tournaisis area through geophysical methods – an overview. *Geol Belg* 17: 17–26.

Klimchouk A, Auler AS, Bezerra FHR, Cazarin CL, Balsamo F, Dublyansky Y. 2016. Hypogenic origin, geologic controls and functional organization of a giant cave system in Precambrian carbonates, Brazil. *Geomorphology* 253: 385–405.

La Bruna V, Bezerra FHR, Souza VHP, Maia RP, Auler AS, Araujo REB, *et al*. 2021. High-permeability zones in folded and faulted silicified carbonate rocks – implications for karstified carbonate reservoirs. *Mar Pet Geol* 128: 105046.

Lamarche J, Lavenu APC, Gauthier BDM, Guglielmi Y, Jayet O. 2012. Relationships between fracture patterns, geodynamics and mechanical stratigraphy in Carbonates (South-East Basin, France). *Tectonophysics* 581: 231–245.

Larzac Explo. 2021. Traçages du sud Larzac: un premier bilan positif. *LARZAC EXPLO – CELADON*. Available from https://larzacexploceladon.fr/index.php/2021/06/02/tracages-du-sud-larzac-un-premier-bilan-positif/ (last consult: 2023/5/4).

Larzac Explo. 2022. L'aven du Cochon est une cavité "Viscieuse".. Les premiers résultats d'un traçages improbable. *LARZAC EXPLO – CELADON*. Available from https://larzacexploceladon.fr/index.php/2022/05/06/laven-du-cochon-est-une-cavite-viscieuse-les-premiers-resultats-du-tracage/ (last consult: 2023/5/4).

Larzac Explo. 2023. La Vis et la Lergue reliées par les eaux souterraines! *LARZAC EXPLO – CELADON*. Available from https://larzacexploceladon.fr/index.php/2023/02/17/la-vis-et-la-lergue-reliees-par-les-eaux-souterraines/ (last consult: 2023/5/4).

Larzac Explo Celadon. 2023. Topographies. *LARZAC EXPLO – CELADON*. Available from https://larzacexploceladon.fr/index.php/topographies/ (last consult: 2023/5/4).

Li Y, Sun J, Wei H, Song S. 2019. Architectural features of fault-controlled karst reservoirs in the Tahe oilfield. *J Pet Sci Eng* 181: 106208.

Lopez M. 1992. Dynamique du passage d'un appareil terrigène a une plateforme carbonatée en domaine semi-aride: le Trias de Lodève, sud de la France, Doctorat, Montpellier: Montpellier II, 402 p.

Loucks RG. 2007. A review of coalesced, collapsed-paleocave systems and sssociated suprastratal deformation. *Acta Carsologica* 36. DOI: 10.3986/ac.v36i1.214. Available from http://ojs.zrc-sazu.si/carsologica/article/view/214 (last consult: 2023/17/1)

Luo L, Liang X, Ma B, Zhou H. 2021. A karst networks generation model based on the anisotropic Fast Marching algorithm. *J Hydrol* 600: 126507.

Malagò A, Efstathiou D, Bouraoui F, Nikolaidis NP, Franchini M, Bidoglio G, *et al*. 2016. Regional scale hydrologic modeling of a karst-dominant geomorphology: The case study of the Island of Crete. *J Hydrol* 540: 64–81.

Malcles O, Vernant P, Chéry J, Ritz J-F., Cazes G, Fink D. 2020. Âges d'enfouissement, fantômes de roches et structuration karstique, cas de la vallée de la Vis (Sud de la France). *Géomorphol: Relief Process Environ* 26: 255–264.

Mangin A. 1975. Contribution à l'étude hydrodynamique des aquifères karstiques, Doctorat, Dijon: Université de Dijon, 267 p.

Marchand E. 2019. Rôle des interactions tectonique-sédimentation sur l'évolution et la variabilité spatiale d'un gisement de bauxite karstique: exemple au bassin de Villeveyrac (Sud de la France), Doctorat, IMT Mines Alès, 284 p.

Marchand E, Séranne M, Bruguier O, Vinches M. 2021. LA-ICP-MS dating of detrital zircon grains from the Cretaceous allochthonous bauxites of Languedoc (south of France): Provenance and geodynamic consequences. *Basin Res* 33: 270–290.

Marza P. 1995. Caractérisation du signal eustatique haute fréquence sur une plateforme carbonatée péritidale, exemple du Lias des Causses, Sud de la France, Doctorat, Montpellier: Montpellier II, 212 p.

Masse JP, Philip J. 1976. Paléogéographie et tectonique du Crétacé Moyen en Provence: Révision du concept d'isthme durancien. *Revue de Géographie Physique et de Géologie Dynamique* 18: 49–66.

Mathbout S, Lopez-Bustins JA, Royé D, Martin-Vide J. 2021. Mediterranean-scale drought: regional datasets for exceptional meteorological drought events during 1975- 2019. *Atmosphere* 12: 941.

Nelson RA. 1979. Natural fracture systems: description and classification. *Am Assoc Pet Geol Bull* 63: 2214–2232.

Palmer AN. 2003. Speleogenesis in carbonate rocks. *Speleogenesis and Evolution of Karst Aquifers The Virtual Scientific J* 1: 1–11.

Paloc H. 1972. Carte hydrogéologique de la région des Grands Causses – Notice explicative. Atlas hydrogéologique du Languedoc-Roussillon. BRGM, 82 p.

Parizot O, Missenard Y, Vergely P, Haurine F, Noret A, Delpech G, *et al*. 2020. Tectonic record of deformation in intraplate domains: case study of far-field deformation in the grands causses area, France. *Geofluids* 2020: 1–19.

Peyaud J-B., Barbarand J, Carter A, Pagel M. 2005. Mid-Cretaceous uplift and erosion on the northern margin of the Ligurian Tethys deduced from thermal history reconstruction. *Int J Earth Sci* 94: 462–474.

Philip H, Bodeur Y, Mattei J, Mattauer M, Therond R, Paloc H, *et al*. 1978. Feuille de St-Martin-de-Londres n°963. Carte géologique de la France au 1/50000. BRGM.

Pinault J-L., Plagnes V, Aquilina L, Bakalowicz M. 2001. Inverse modeling of the hydrological and the hydrochemical behavior of hydrosystems: Characterization of Karst System Functioning. *Water Resour Res* 37: 2191–2204.

Pisani L, Antonellini M, Bezerra FHR, Carbone C, Auler AS, Audra P, *et al*. 2022. Silicification, flow pathways, and deep-seated hypogene dissolution controlled by structural and stratigraphic variability in a carbonate-siliciclastic sequence (Brazil). *Mar Pet Geol* 139: 105611.

Pontes CCC, Bezerra FHR, Bertotti G, La Bruna V, Audra P, De Waele J, *et al*. 2021. Flow pathways in multiple-direction fold hinges: Implications for fractured and karstified carbonate reservoirs. *J Struct Geol* 146: 104324.

Quinif Y. 1998. Dissipation d'énergie et adaptabilité dans les systèmes karstiques. *Karstologia* 31: 1–11.

Quinif Y. 1999. Fantômisation, cryptoaltération et altération sur roche nue, le triptyque de la karstification. *Proceedings of the Colloque européen Karst 99 European Conference*. University of Provence; pp. 159-164.

Quinif Y. 2017. Les couloirs endokarstiques: Elements structurants d'une cavité. *Karstologia* 69: 29–32.

Quinif Y, Baele J-M., Dubois C, Havron C, Kaufmann O, Vergari A. 2014. Fantômisation: un nouveau paradigme entre la théorie des deux phases de Davis et la théorie de la biorhexistasie d'Erhart. *Geol Belg* 17: 66–74.

Quinif Y, Bruxelles L. 2011. L'altération de type «fantôme de roche»: processus, évolution et implications pour la karstification. *Géomorphol: Relief Process Environ* 17: 349–358.

Quinif Y, Maire R. 2009. La grotte Quentin (Hainaut, Belgique): un modèle d'évolution des fantômes de roche. *Karstologia Mémoires* 18: 214–218.

Quinif Y, Rorive A, Bruxelles L. 2022. Fantômisation et hydrogéologie. *Karstologia Mémoires* IV: 235–238.

Séranne M. 1999. The Gulf of Lion continental margin (NW Mediterranean) revisited by IBS: an overview. *Geol Soc London Spec Publ* 156: 15–36.

Séranne M, Camus H, Lucazeau F, Barbarand J, Quinif Y. 2002. Surrection et érosion polyphasées de la bordure cévenole. Un exemple de morphogenèse lente. *Bulletin de la Société Géologique de France* 173: 97–112.

SpéléoClub de Lodève-Groupe Vallot. 1985. Recherche de l'exutoire de la cavité de l'Aven du Saut du Lièvre . Available from https://fichetracages.brgm.fr/fichetracage?idtracage=8164

Tičar J. 2015. Geomorphological characteristics of selected pocket valleys in Slovenia. *Geografski Vestnik* 87: 23–42.

Tognini P, Bini A. 2001. Effects of the structural setting on endokarst system geometry in the Valle del Nosê (Como Lake, Northern Italy). *Geol Belg* 4: 197–211.

Tritz S, Guinot V, Jourde H. 2011. Modelling the behaviour of a karst system catchment using non-linear hysteretic conceptual model. *J Hydrol* 397: 250–262.

Vergari A. 1998. Nouveau regard sur la spéléogenèse: le "pseudo-endokarst" du Tournaisis (Hainaut, Belgique). *Karstologia* 31: 12–18.

Vergari A, Quinif Y. 1997. Les paléokarsts du Hainaut (Belgique). *Geodinamica Acta* 10: 175–187.

Vernant P, Malcles O, Fink D, Cazes G. 2022. Regional karst network genesis due to removal of ghost rocks revealed by burial dating. *Proceedings of the UIS*. Savoie Mont Blanc, pp. 239-242.

Vicente-Serrano SM, Lopez-Moreno J-I., Beguería S, Lorenzo-Lacruz J, Sanchez-Lorenzo A, García-Ruiz JM, *et al*. 2014. Evidence of increasing drought severity caused by temperature rise in southern Europe. *Environ Res Lett* 9: 044001.

Cite this article as: Baral C, Séranne M, Camus H, Jouves J. 2024. Impact of alteration corridors on karst reservoir organisation and evolution of groundwater flow path: An example from the southern border of the Larzac Causse, southern France, *BSGF - Earth Sciences Bulletin* 195: 4.